

Spring 2024

Cross-Layer Performance Evaluation of C-V2X

Dhruba Sunuwar

Follow this and additional works at: <https://digitalcommons.georgiasouthern.edu/etd>



Part of the [Systems and Communications Commons](#)

Recommended Citation

Sunuwar, Dhruba, "Cross-Layer Performance Evaluation of C-V2X" (2024). *Electronic Theses and Dissertations*. 2774.

<https://digitalcommons.georgiasouthern.edu/etd/2774>

This thesis (open access) is brought to you for free and open access by the Jack N. Averitt College of Graduate Studies at Georgia Southern Commons. It has been accepted for inclusion in Electronic Theses and Dissertations by an authorized administrator of Georgia Southern Commons. For more information, please contact digitalcommons@georgiasouthern.edu.

CROSS-LAYER PERFORMANCE EVALUATION OF C-V2X

by

DHRUBA SUNUWAR

(Under the Direction of Seungmo Kim)

ABSTRACT

The evolution of connected vehicles from a distant futuristic concept to an integral part of daily life is indisputable. Vehicle-to-everything communication (V2X) serves as the cornerstone of this transformation, facilitating seamless interaction among vehicles, infrastructure, pedestrians, and networks. However, evaluating V2X system performance proves intricate due to the dynamic nature of vehicles influenced by mobility factors. To address this complexity, we have developed a specialized system-level simulator expressly for evaluating V2X communication performance. Notably, the simulator encompasses (i) intelligent transportation system (ITS) scenarios integrated into a geographical framework and (ii) the capability to assess cross-layer performance spanning physical (PHY) and radio resource control (RRC) aspects. Recent decisions by the United States federal government to reallocate spectrum bands, particularly the "5.9 GHz band" previously allocated to V2X, have raised concerns within the CV2X community. With only 40% of the original bandwidth retained for V2X communication (equivalent to 30 MHz), doubts arise regarding the adequacy of this spectrum allocation to support critical V2X safety messages and applications. To address these concerns systematically, we conduct a comprehensive

investigation into various types of safety messages and their corresponding latency requirements. This investigation encompasses analyses of Packet Delivery Rates (PDR) and latency under diverse vehicular densities and quantities of Road Side Units (RSUs). Consequently, the study presents simulation outcomes scrutinizing the feasibility of meeting these requirements within the constraints of the 30-MHz spectrum configuration. Furthermore, given the prevalence of significant obstacles and high traffic density in urban city road environments, an in-depth analysis of vehicle performance under different Modulation and Coding Schemes (MCS) is imperative. These analyses are pivotal for ensuring the continued effectiveness and reliability of V2X systems amidst evolving regulatory landscapes and technological advancements in the realm of connected vehicles.

INDEX WORDS: Connected vehicles, C-V2X, Latency, Modulation and Coding Schemes (MCS), Packet Delivery Rate (PDR), 5.9 GHz

CROSS-LAYER PERFORMANCE EVALUATION OF C-V2X

by

DHRUBA SUNUWAR

B.E., Tribhuvan University, Nepal, 2016

A Dissertation Submitted to the Graduate Faculty of Georgia Southern University

in Partial Fulfillment of the Requirements for the Degree

MASTER OF SCIENCE

ALLEN E PAULSON COLLEGE OF ENGINEERING AND COMPUTING

STATESBORO, GEORGIA

© 2024

DHRUBA SUNUWAR

All Rights Reserved

CROSS-LAYER PERFORMANCE EVALUATION OF C-V2X

by

DHRUBA SUNUWAR

Major Professor: Seungmo Kim

Committee: Sungkyun Lim

Rami J. Haddad

Electronic Version Approved:

May 2024

DEDICATION

This project is a tribute to my parents, brother, and beloved wife, who have always been there for me, offering constant support and trust. Their encouragement has been the driving force behind my efforts, guiding me through every step of this journey. Without their unwavering belief in me, I wouldn't have had the courage or determination to see this project through to completion. I owe a debt of gratitude to my wife, whose steady support and numerous sacrifices have been crucial to my success. Her presence has been a source of strength and inspiration, motivating me to overcome challenges and keep pushing towards my goals.

ACKNOWLEDGMENTS

My pursuit of a master's degree was greatly facilitated by Dr. Seungmo Kim, who served as an exceptional mentor and a humble supervisor. I am deeply grateful to him for consistently trusting, encouraging, supporting, guiding, and explaining all the intricacies of the research process. Additionally, I extend my gratitude to my thesis committee members, Dr. Rami J. Haddad, and Dr. Sungkyun Lim, for dedicating their time and offering valuable insights and constructive suggestions. I also want to express appreciation to Ms. Tiffany Courdin for her prompt assistance with the administrative tasks associated with maintaining my research assistantship position. Furthermore, I am thankful to my brother, Suresh Sunuwar, for his assistance in improving and refining this report to ensure its quality and professionalism. My time at Georgia Southern University over the past two and a half years has been enriching and transformative, providing me with an invaluable platform for personal and academic growth. Therefore, I extend sincere gratitude to the university community for their support and contributions to my development.

TABLE OF CONTENTS

	Page
ACKNOWLEDGMENTS	3
LIST OF TABLES	6
LIST OF FIGURES	7
CHAPTER 1	10
INTRODUCTION	10
1.1 Background	10
1.2 Motivation	11
1.3 Related Work	12
1.4 Contributions	13
CHAPTER 2	14
LITERATURE REVIEW	14
2.1 Cellular Vehicle to Everything Communications (C-V2X)	14
2.2 UMi-Street Canyon Pathloss Model	25
2.3 Modulation and Coding Scheme (MCS)	27
2.4 ITS Message Types	28
2.5 Performance Metrics	30
CHAPTER 3	32
SYSTEM MODEL	32

3.1	Spatial Environment Simulator.....	32
3.2	LTE-V2X Simulator Communication Parameters.....	37
3.3	Conditions for Dropping Packets.....	38
3.4	Mapping SNR and BER.....	39
3.5	Algorithms and Flowcharts.....	42
CHAPTER 4.....		49
RESULTS AND DISCUSSION.....		49
4.1	Key Parameters for Simulation.....	49
4.2	RSU-to-Vehicle Latency.....	52
4.3	Packet Delivery Rate (PDR).....	65
4.4	PDR vs Distance from RSU.....	72
CHAPTER 5.....		75
CONCLUSION AND FUTURE WORK.....		75
REFERENCES.....		77

LIST OF TABLES

	Page
Table 1. CR Limit Values (<i>ETSI TS 136 331, 2018</i>).	23
Table 2. Mapping of Message Types to Traffic Priority Levels (<i>SAE J2745, 2020</i>).	29
Table 3. Key Parameters for Simulation with Setting 1.	50
Table 4. Key Parameters for Simulation with Setting 2.	51

LIST OF FIGURES

	Page
Figure 1. C-V2X Spectrum Reallocation (<i>www.westernsystems-inc.com</i>).....	12
Figure 2. C-V2X Ecosystem Showing V2V, V2I, V2P, and V2C (<i>Hope Bovenzi, 2019</i>)	15
Figure 3. Resource Grid Structure in Time and Frequency Domains (<i>Sabeeh, et al., 2022</i>)	17
Figure 4. LTE-V2X Subchannel Configurations. (a) Adjacent PSSCH + PSCCH (b) Nonadjacent PSSCH + PSCCH (<i>M. Garcia et al., 2022</i>)	18
Figure 5. Mode 3 and Mode 4 Defined in Release 14 (<i>Gupta, et al., 2019</i>).....	18
Figure 6. Sensing and Selection Window (<i>Ghodhbane, et al., 2022</i>).....	21
Figure 7. CBR and CR Calculations in DCC Mechanisms (<i>Mansouri, et al., 2019</i>)	21
Figure 8. Definition of $d2D$ and $d3D$ for Outdoor User Terminals (UTs) (<i>3GPP, 2022</i>)	26
Figure 9. Geometrical Setup of the Proposed Simulator (with Vehicle Density of $\lambda = 2$ in the Entire System Space \mathbb{R}^2)	33
Figure 10. Number of Vehicles for $\lambda = \{10, 20\}$	35
Figure 11. Connection Links with Vehicles when # RUS = $\{1,2\}$ and $\lambda = 2$	36
Figure 12. SNR vs BER Mapping Using MATLAB Built-In Functions with Payload (a) 190 bytes (b) 300 bytes (c) 500 bytes.....	40
Figure 13. Basic Flowchart of the Overall Simulation	41
Figure 14. Distribution of RSU-to-Vehicle Latency and Traffic Density ($\lambda = 10$) Compared to Latency Requirements of 20 msec as Red Vertical Line. (a) RSU = 1 (b) RSU = 2 (c) RSU = 3	54
Figure 15. Distribution of RSU-to-Vehicle Latency and Traffic Density ($\lambda = 20$) Compared to Latency Requirements of 20 msec as Red Vertical Line. (a) RSU = 1 (b) RSU = 2 (c) RSU = 3	55

Figure 16. Distribution of RSU-to-Vehicle Latency and Traffic Density ($\lambda = 30$) Compared to Latency Requirements of 20 msec as Red Vertical Line. (a) RSU = 1 (b) RSU = 2 (c) RSU = 3	56
Figure 17. Distribution of RSU-to-Vehicle Latency (Congestion Control Mechanism Enabled) and Traffic Density ($\lambda = 30$), Compared to Latency Requirements of 20 msec as Red Vertical Line. (a) RSU = 1 (b) RSU = 2 (c) RSU = 3	59
Figure 18. Distribution of RSU-to-Vehicle Latency (Congestion Control Mechanism Disabled) and Traffic Density ($\lambda = 15$) Compared to Latency Requirements of 20 msec as Red Vertical Line. The Mean Vehicle Speed is Set to (a) 6 m/s, (b) 12 m/s, and (c) 24 m/s	61
Figure 19. Distribution of Latency According to MCS Index = {7, 11} (Compared Column-Wise) and Traffic Density = {30, 60} (Compared Row-Wise) Compared to Latency Requirement of 20 msec as Red Vertical Line.....	63
Figure 20. Distribution of Latency According to MCS Index = {7, 11} (Compared Column-Wise) and Traffic Density = {90, 120} (Compared Row-Wise) Compared to Latency Requirement of 20 msec as Red Vertical Line.....	64
Figure 21. Distribution Packet Delivery Rate (PDR) According to Number of RSUs and Traffic Density ($\lambda = 10$) Showing the Mean PDR Values (Indicated by the Green Vertical Line)	66
Figure 22. Distribution Packet Delivery Rate (PDR) According to Number of RSUs and Traffic Density ($\lambda = 20$) Showing the Mean PDR Values (Indicated by the Green Vertical Line)	67

Figure 23. Distribution of PDR According to MCS Index = {7, 11} (Compared Column-Wise) and Traffic Density = {30, 60} (Compared Row-Wise)	70
Figure 24. Distribution of PDR According to MCS Index = {7, 11} (Compared Column-Wise) and Traffic Density = {90, 120} (Compared Row-Wise)	71
Figure 25. PDR Variation for $\lambda = \{5, 10\}$ with Respect to Distance from the RSU where Green Plots Indicate MCS 7 and Blue Plots Indicate MCS 11	73
Figure 26. PDR Variation for $\lambda = \{15, 20\}$ with Respect to Distance from the RSU where Green Plots Indicate MCS 7 and Blue Plots Indicate MCS 11	74

CHAPTER 1

INTRODUCTION

1.1 Background

In today's rapidly growing cities and advancing technology landscape, Cellular Vehicle-to-Everything (C-V2X) technology emerges as a critical solution for enhancing modern transportation systems. Enabling vehicles to communicate with each other, traffic signs, and pedestrians, C-V2X facilitates real-time sharing of vital information such as road conditions, traffic congestion, and potential hazards. This empowers vehicles to make informed decisions swiftly, enhancing overall road safety and efficiency. Moreover, C-V2X aids in reducing traffic congestion by providing vehicles with route updates and guiding them away from congested areas. Additionally, it facilitates communication with traffic lights and road signs, streamlining traffic flow. Beyond immediate benefits, C-V2X lays the groundwork for future advancements like self-driving cars and smart city initiatives, offering promising solutions to address urban growth and environmental challenges while fostering safer, more efficient, and sustainable transportation systems globally.

Regulating C-V2X technology involves collaboration among governmental bodies, industry consortia, and standards organizations. In the United States, the Federal Communications Commission (FCC) allocates spectrum and sets deployment rules, while the National Highway Traffic Safety Administration (NHTSA) ensures safety standards compliance. Internationally, entities like the European Telecommunications Standards Institute (ETSI) and the 3rd Generation Partnership Project (3GPP) establish global communication protocols. Automotive industry leaders, such as Qualcomm, Ford, and BMW, actively contribute to regulatory processes, advocating for C-V2X adoption. This

collaborative effort is crucial for innovation, safety, and the seamless integration of C-V2X technology into the transportation ecosystem.

1.2 Motivation

V2X technology facilitates communication among vehicles, infrastructure, and vulnerable road users, enhancing safety and averting traffic accidents, fatalities, congestion, and environmental impacts (USDOT 2017). This pivotal role places V2X communications at the heart of intelligent transportation systems (ITS) for connected vehicle environments. Traditionally, the entire 75 MHz bandwidth of the 5.9 GHz spectrum band (5.850-5.925 GHz) has been earmarked for intelligent transportation services like V2X technologies. However, the U.S. Federal Communications Commission (FCC) recently decided to allocate the lower 45 MHz (i.e., 5.850-5.895 GHz) for unlicensed operations to support broadband applications as highlighted in Figure 1, such as Wi-Fi (U.S. FCC 2019). Furthermore, the upper 30 MHz (i.e., 5.895-5.925 GHz) has been designated solely for cellular V2X (C-V2X) to support ITS. Consequently, it is imperative to evaluate the potential within this limited 30 MHz spectrum to ensure the continued development and deployment of traffic safety applications by ITS stakeholders.

Additionally, the standardization efforts outlined in SAE J3161 (SAE, 2022) do not cover the investigation into how vegetation lining streets, avenues, and parkways, as well as the presence of scaffolding and other obstructions, impact the operational range, in addition to occlusion by larger vehicles such as 18-wheel trailers and garbage trucks. Consequently, addressing this concern is imperative.

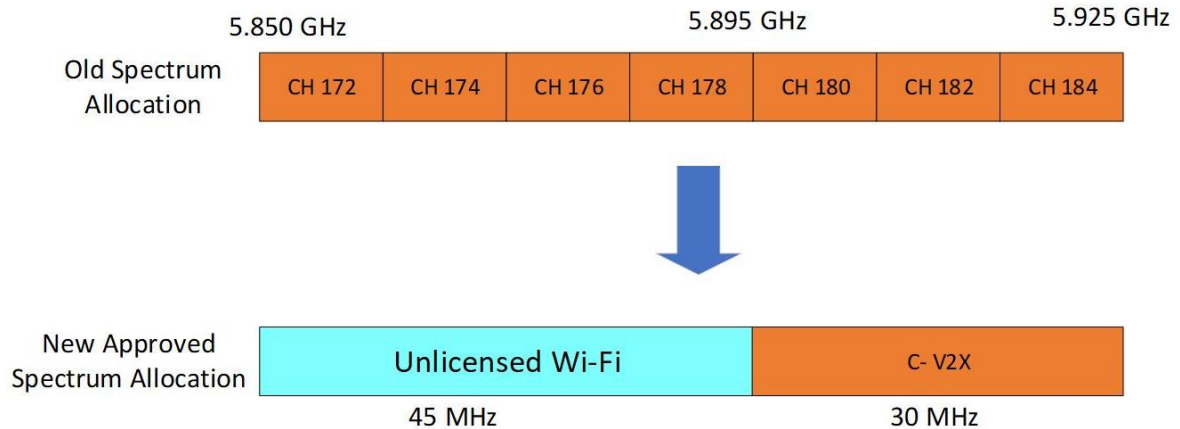


Figure 1. C-V2X Spectrum Reallocation (www.westernsystems-inc.com)

1.3 Related Work

It is evident that C-V2X has garnered substantial attention within academic literature. However, scant consideration has been given to its feasibility within the constrained 30 MHz spectrum allocated for safety applications. While much emphasis has been placed on per-packet latency, denoting the time taken for a packet to traverse from its origin to its destination, an additional metric, namely the inter-reception time (IRT), has been proposed to measure the duration between successful packet deliveries (T. E. Batt et al., 2006). Yet, the IRT's utility appears limited, particularly in broadcast-based safety applications. Given the diverse range of applications under consideration, this thesis predominantly employs Packet Delivery Rate (PDR) and conventional latency as the principal metrics, as elaborated in the chapters followed by. Various proposals have been posited in the literature to delineate V2X systems, encompassing theoretical or mathematical approaches (L. Cao et al. 2022), simulations (R. Wei 2022), and channel sounding (M. Akdeniz et al. 2014). While these studies offer valuable insights, they fall short of conclusively determining whether the

reduced 30-MHz bandwidth can adequately support C-V2X in practical road and traffic scenarios. A similar gap is apparent in current research on V2X safety applications (C. Zoghiami et al. 2022), where proposals outline methods to bolster such applications but fail to address the ramifications of a 60% bandwidth reduction for C-V2X.

1.4 Contributions

This study serves as an initial exploration intended to stimulate discourse within the ITS literature regarding the implementation of C-V2X technologies in such conditions. Rather than definitive or conclusive, this effort should be seen as a catalyst, prompting further investigations and evaluations into the effects of the 30 MHz environment on application deployment. With this in mind, we contribute to the C-V2X literature in the following ways:

- Pioneering efforts to elucidate the viability of safety-critical applications within the reduced 30 MHz spectrum setting.
- Developing a framework for quantifying C-V2X performance in a comprehensive yet accessible manner.
- Demonstrating the accuracy of outcomes produced by the simulator framework, which encompasses: (i) ITS scenarios in various geographic and traffic configurations and (ii) the capability for cross-layer performance evaluation in PHY/RRC.
- Identifying message types relevant to safety-critical applications.

CHAPTER 2

LITERATURE REVIEW

2.1 Cellular Vehicle to Everything Communications (C-V2X)

2.1.1. Introduction to C-V2X

The landscape of transportation is undergoing a profound transformation with the advent of Cellular Vehicle-to-Everything (C-V2X) communication technology. This revolutionary advancement holds the promise of fundamentally reshaping how vehicles interact with each other, infrastructure, pedestrians, and the broader transportation ecosystem. C-V2X enables vehicles to communicate seamlessly with their surroundings, paving the way for enhanced safety, improved traffic efficiency, and an unparalleled driving experience.

C-V2X technology operates on cellular networks, leveraging both direct communication (between vehicles and infrastructure) and network-based communication (between vehicles and the cloud). This dual-mode capability ensures robust connectivity in various driving scenarios, including urban environments, highways, and rural areas. Unlike its predecessors, Dedicated Short-Range Communication (DSRC), C-V2X doesn't rely solely on line-of-sight communication, offering extended range and enhanced reliability. The significance of C-V2X lies in its ability to facilitate advanced safety features that mitigate the risk of accidents and improve overall road safety. By exchanging real-time data on vehicle speed, position, and surrounding road conditions, C-V2X enables features such as cooperative adaptive cruise control, intersection collision warnings, and emergency brake assistance. Moreover, C-V2X empowers vehicles to anticipate and react to potential hazards

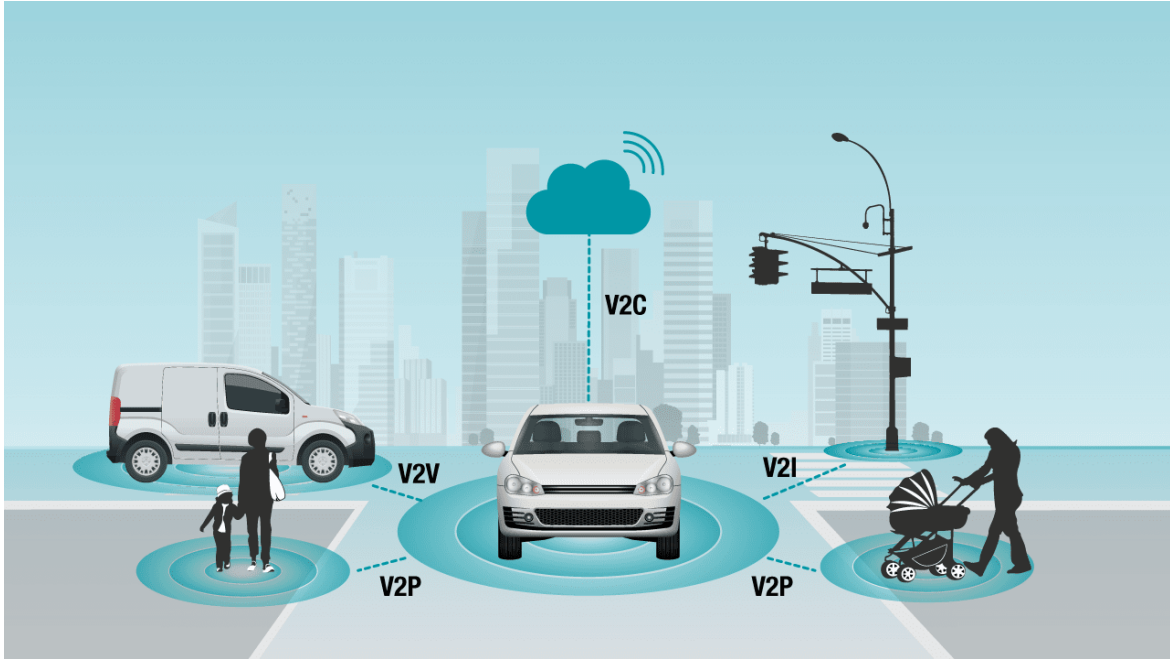


Figure 2. C-V2X Ecosystem Showing V2V, V2I, V2P, and V2C (*Hope Bovenzi, 2019*)

more effectively, reducing the likelihood of collisions and enhancing the safety of all road users. Beyond safety, C-V2X technology holds immense potential for optimizing traffic flow and alleviating congestion on roadways. Through cooperative traffic management systems, vehicles equipped with C-V2X can receive real-time traffic information, optimize route planning, and adapt their driving behavior to minimize delays and maximize efficiency. This capability not only improves the overall driving experience for individuals but also contributes to reducing fuel consumption and greenhouse gas emissions on a larger scale.

Real-world trials and pilot projects demonstrate the feasibility and effectiveness of C-V2X which are branched into four different pillars as illustrated in Figure 1, namely, vehicle-to-vehicle (V2V) communication, vehicle-to-infrastructure (V2I) communication, vehicle-to-network/cloud (V2N/V2C) communication, and vehicle-to-pedestrian (V2P) communication. As C-V2X continues to evolve and mature, it is poised to play a central role

in shaping the future of transportation. However, realizing its full potential requires addressing technical, regulatory, and societal challenges, including interoperability, spectrum allocation, privacy concerns, and public acceptance. Through collaborative efforts across industry stakeholders, policymakers, and the research community, C-V2X holds the promise of creating safer, smarter, and more sustainable transportation systems for generations to come.

2.1.2. Resource Allocation in LTE-V2X Communications through Mode 4

In LTE-V2X, like LTE up-link, the physical layer utilizes OFDM while the MAC layer employs Single-Carrier Frequency Division Multiple Access (SC-FDMA). The available bandwidth, whether it's a 10 or 20 MHz channel, is divided into orthogonal resources in both time and frequency domains as shown in Figure 3. In the time domain, signals are organized into frames of 10 ms, each consisting of 10 sub-frames of 1 ms each, further divided into 2 Time-Slots. In the frequency domain, Resource Block Pairs (RBPs) define the signal, comprising 12 sub-carriers spaced by 15 kHz, each carrying 14 OFDM symbols. For LTE-V2X, a sub-channel is a group of RBPs within a sub-frame, with configurable sizes ranging from 4 to 50 RBPs, although all subchannels within an Evolved Node B (eNB) must be the same size. Vehicles can utilize one or multiple subchannels to transmit their data, with each sub-channel representing the smallest unit of resource assigned for transmitting CAM packets.

In C-V2X, modulation is achieved using Quadrature Phase Shift Keying (QPSK) and 16QAM for Transport Blocks (TBs), while Sidelink Control Information (SCI) is consistently transmitted using QPSK. Turbo coding and the normal cyclic prefix are utilized

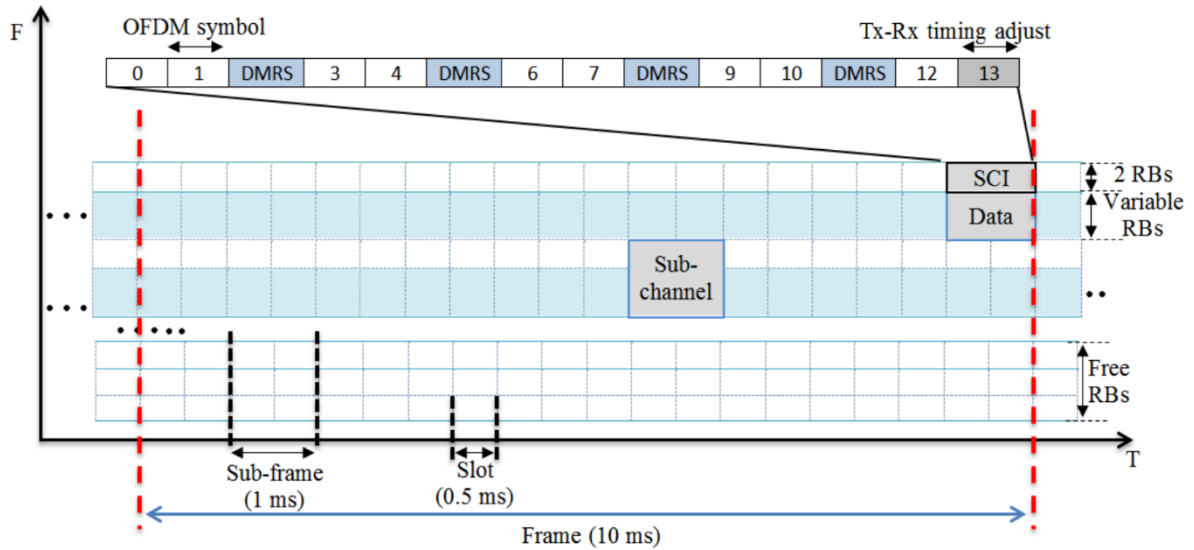


Figure 3. Resource Grid Structure in Time and Frequency Domains (*Sabeeh, et al., 2022*)

in LTE-V2X. Transport Channel (TCH) data transmission is facilitated by the Physical Sidelink Shared Channel (PSSCH), while the Physical Sidelink Control Channel (PSCCH) conveys SCI. The SCI includes critical information such as MCS data, occupied RBs by the associated TB, message priority, and resource reservation interval, vital for successful message decoding at the receiver. The resource reservation interval specifies when the vehicle will utilize reserved resources for its subsequent transmission.

PSCCH and PSSCH are multiplexed in the frequency domain, being transmitted within the same sub-frame but utilizing different frequency resources. There are two configuration schemes for PSSCH and PSCCH: adjacent configuration, where PSCCH occupies the first two RBs of the allocated sub-channel, directly followed by PSSCH, and non-adjacent configuration, where PSSCH and PSCCH do not occupy consecutive RBs within the same sub-frame as shown in Figure 4. The number of RBs in a sub-channel remains variable in this study depending upon the Congestion Control Mechanism being enabled/disabled and the chosen MCS index.

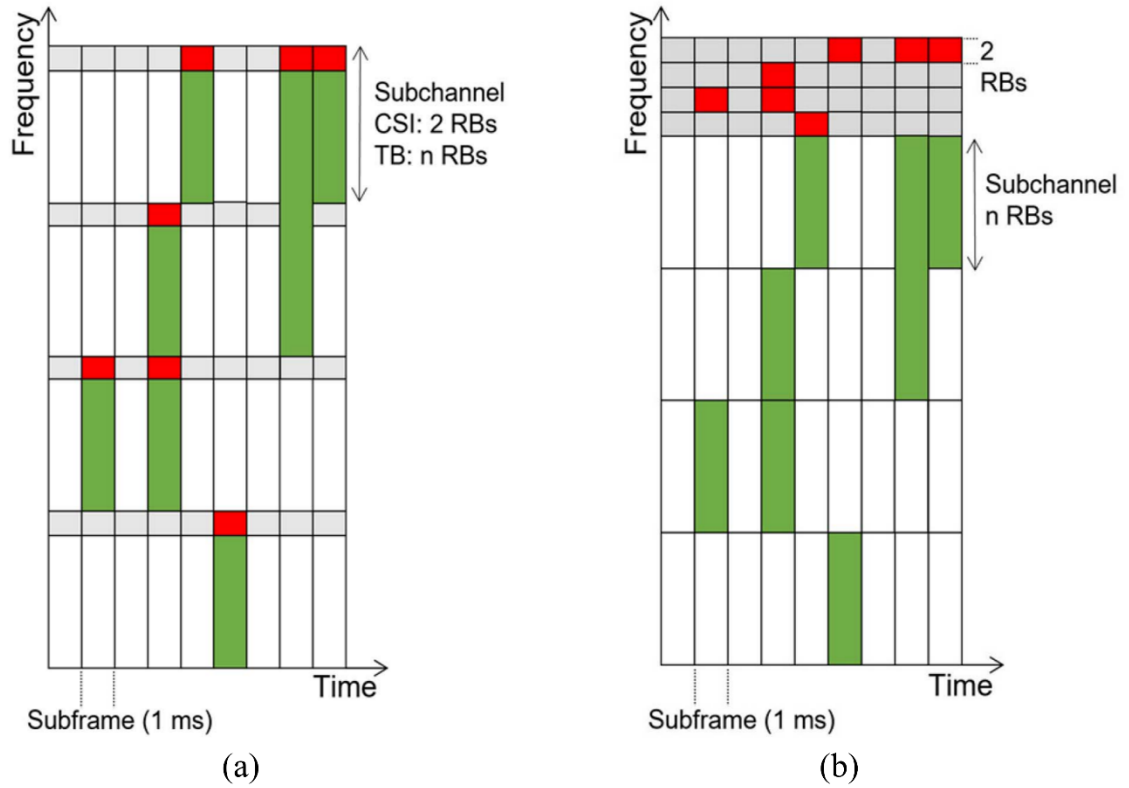


Figure 4. LTE-V2X Subchannel Configurations. (a) Adjacent PSSCH + PSCCH
 (b) Nonadjacent PSSCH + PSCCH (*M. Garcia et al., 2022*)

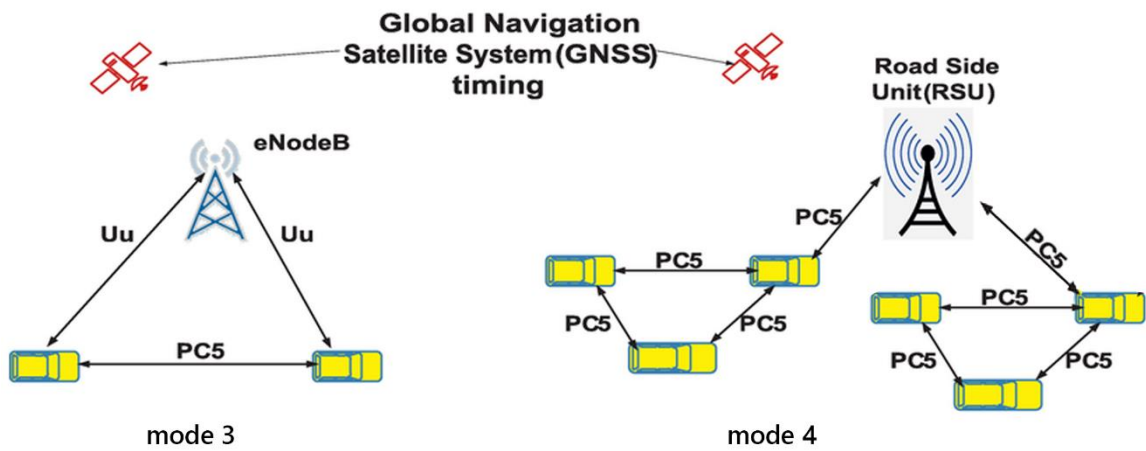


Figure 5. Mode 3 and Mode 4 Defined in Release 14 (*Gupta, et al., 2019*)

LTE-V2X introduces two resource allocation modes, as depicted in Figure 5, which correspond to the availability of cellular infrastructure. The first mode, known as mode 3, operates within cellular coverage, where the eNB orchestrates resource scheduling and allocation to vehicles. However, to ensure the provision of basic safety services even when vehicles venture beyond cellular coverage, 3GPP has standardized a second mode, referred to as mode 4. Under mode 4, vehicles autonomously determine their radio resources utilizing the SPS algorithm. This algorithm hinges on channel sensing before selecting a resource from a pool of candidate resources, as elaborated upon subsequently.

2.1.3. Sensing-Based Semi-Persistent Scheduling

Mode 4, as standardized by 3GPP, entails autonomous radio resource selection for vehicles. In this mode, vehicles autonomously determine their radio resources using the SPS algorithm, elaborated further in (Gonzalez-Martín et al., 2018 and Molina-Masegosa et al., 2017). The SPS operates on the principle of sensing before resource selection from a list of candidate resources, with the following fundamental principles:

- Upon reserving a resource, a vehicle utilizes it to transmit a variable number of consecutive messages. This number, termed the re-selection counter (RC), is contingent on the periodicity of CAM messages. For instance, for a periodicity of 10 Hz, the re-selection counter ranges from 5 to 15; for 20 Hz, it ranges from 10 to 30, and for 50 Hz, it extends from 25 to 75.
- The periodicity of CAM messages and the re-selection counter's value are embedded in the SCI field. Consequently, based on this information, vehicles discern available and occupied resources.

- After each CAM message transmission, the re-selection counter decrements by 1. Upon reaching zero, a new resource selection becomes imperative with a probability of $(1 - P)$, where P denotes the probability of retaining the current resource for subsequent transmissions.

The operation of the SPS algorithm can be segmented into three primary steps, as depicted in Figure 6. In the initial step, the vehicle earmarks candidate resources within a designated Selection Window (SW). The SW constitutes a time interval defined by $[n + T1, n + T2]$, where T denotes the subframe at which the vehicle intends to designate a new candidate resource. $T1$ represents the processing time (in subframes) required by a vehicle to identify and nominate candidate resources for transmission, bounded by $1 \leq T1 \leq 4$. $T2$ is also determined by the vehicle and must fall within the range of $20 \leq T2 \leq 100$. Subsequently, the vehicle monitors the channel during the "Sensing Window" for a duration of 1 second. The Sensing Window corresponds to the most recent 1,000 subframes. Figure 6 illustrates the sensing and selection windows for the SPS algorithm.

In the subsequent step, the vehicle compiles an initial list, termed LI , comprising the resources previously selected during the selection window, excluding those exhibiting a Reference Signal Received Power (RSRP) level surpassing a specified power threshold, denoted as Th . Additionally, LI omits resources occupied by other vehicles for their forthcoming transmissions, based on SCI information. This list must encompass at least 20% of the total resources selected in the initial step. If not, this step is reiterated iteratively, increasing the power threshold Th by 3 dB with each iteration.

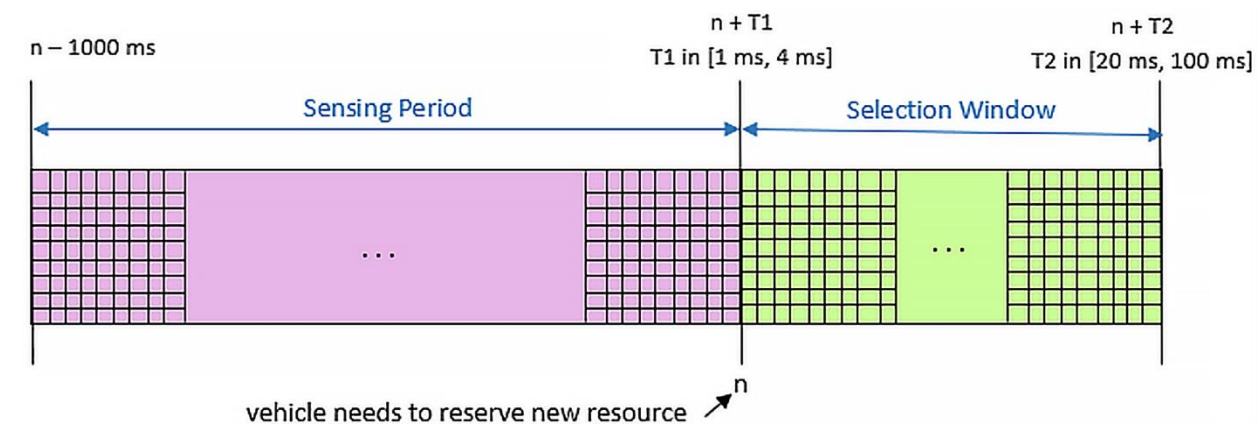


Figure 6. Sensing and Selection Window (Ghodhbane, et al., 2022)

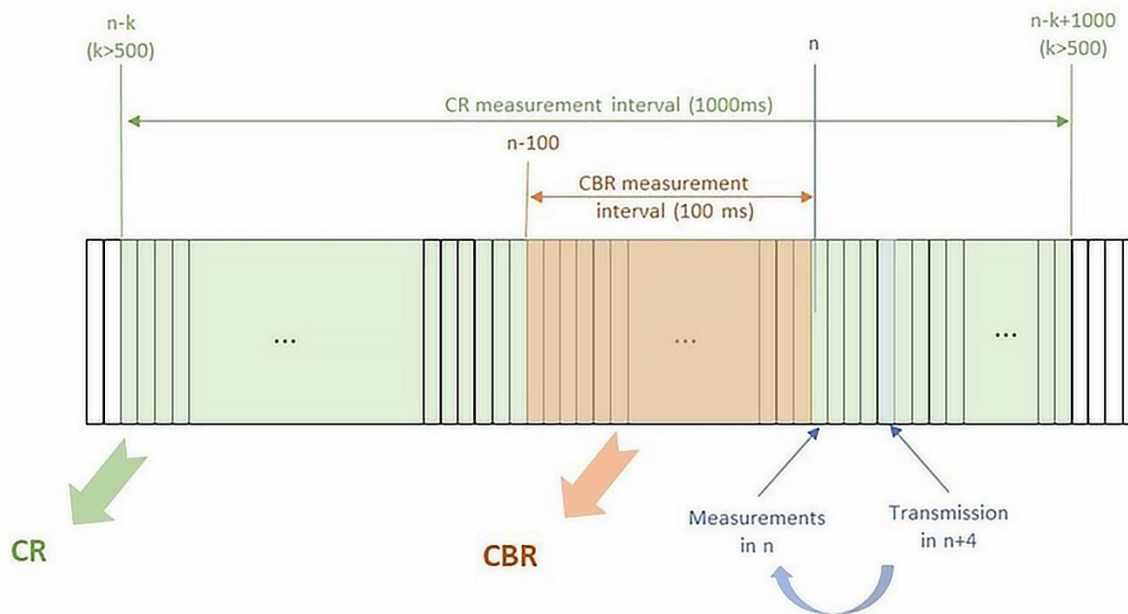


Figure 7. CBR and CR Calculations in DCC Mechanisms (Mansouri, et al., 2019)

In the final step, the vehicle generates a list of resources, denoted as $L2$, showcasing the minimum Received Signal Strength Indication (RSSI) values. The count of these resources must equate to 20% of the total resources selected in the initial step. Consequently, the vehicle randomly selects a definitive resource from the $L2$ list and reserves this resource according to its re-selection counter for subsequent transmissions. This random selection mitigates collision risks in scenarios where two vehicles opt for the same resource, presenting the lowest RSSI value.

LTE-V2X Congestion Control Mechanism

In dense scenarios, a substantial number of LTE-V2X stations may coexist within a confined geographical area, thereby presenting challenges in resource sharing. Consequently, the implementation of Decentralized Congestion Control (DCC) is essential to coordinate channel usage (Mansouri, et al., 2019). All stations are required to collaborate to maintain an unsaturated channel, ensuring equitable resource allocation. The LTE-V2X standard defines two metrics to characterize channel state and guide stations in taking necessary actions: the channel busy ratio (CBR) and the channel occupancy ratio (CR), as depicted in Figure 7.

- **Channel busy ratio (CBR):** This metric is defined as the proportion of subchannels in the resource pool whose Received Signal Strength Indication (RSSI) measurement exceeds a predetermined threshold. The CBR is evaluated over the most recent 100 subframes, offering an estimation of the overall channel state.
- **Channel occupancy ratio (CR):** Calculated at subframe n , the CR represents the total number of subchannels utilized for transmissions within subframes $[n-a, n-1]$, and those

allocated in subframes $[n, n+b]$, divided by the total number of subchannels within the range $[n-a, n+b]$. The values of a and b are determined by the station, with the constraint that their sum equals 1000, and a being greater than or equal to 500. The CR provides an indication of channel utilization by the transmitter itself.

Within the simulator, the Channel Busy Ratio (CBR) undergoes measurement every 10 milliseconds, subsequently leading to adjustments of the Channel Occupancy Ratio (CR) limits. These adjustments ensure alignment with the designated CR limit values outlined in Table 1.

Table 1. CR Limit Values (*ETSI TS 136 331, 2018*).

CBR-based PSSCH transmission parameter configuration	PPPP1-PPPP2	PPPP3-PPPP5	PPPP6-PPPP8
CBR measured	CR limit	CR limit	CR limit
$0 \leq \text{CBR measured} \leq 0.3$	No limit	No limit	No limit
$0.3 < \text{CBR measured} \leq 0.65$	No limit	0.03	0.004
$0 < \text{CBR measured} \leq 0.8$	0.02	0.006	0.02
$0 < \text{CBR measured} \leq 1$	0.02	0.003	0.002

LTE-V2X Adaptive Mechanisms

CBR and CR measurements are updated after each subframe. The CBR range can be divided into up to 16 intervals, with each interval having a corresponding CR limit established as a threshold that the transmitter must not exceed. When an LTE-V2X station

decides to transmit a packet, it maps its CBR value to the appropriate interval to determine the corresponding CR limit value. If the station's CR surpasses the CR limit, it is required to reduce its CR below that limit. The standard does not specify a particular technique for reducing the CR, leaving it to individual implementations to choose from the following options (Mansouri, et al., 2019).

- **Drop packet transmission/retransmission:** The LTE-V2X station simply discards transmitted and retransmitted packets if there is a blockage, if the vehicle is outside the range of the Road Side Unit (RSU), or if the received signal strength falls below the pre-defined threshold. It's important to note that from the LTE-V2X transmitter's perspective, resource reservation for subsequent transmissions is maintained even if a packet is dropped, as long as the re-selection counter has not reached zero.
- **Adapt the MCS:** The LTE-V2X station can reduce its CR by increasing the Modulation and Coding Scheme (MCS) index used. This action can decrease the number of subchannels employed for transmission. However, increasing the MCS index compromises the message's robustness and consequently reduces its range. In this study, MCS index 7 and 11 are considered.
- **Adapt transmission power:** The LTE-V2X station can lower its transmission power, resulting in a reduction in the overall CBR in the vicinity. This adjustment may potentially increase the value of the CR limit. However, due to complexity, this approach has not been implemented in the study.

2.2 UMi-Street Canyon Pathloss Model

Since a city road environment is considered for the study, Urban Micro-Street Canyon Pathloss model (3GPP ETSI TR 1389010) has been implemented in the overall simulation. The pathloss model incorporates all the evaluation parameters such as base station (BS) antenna height, user terminal (UE) height and distance from the RSU, respective antenna models, line-of-sight (LOS) and non-line-of-sight (NLOS) approaches, etc. Equations 1 to 3 give the pathloss (in dB) for LOS scenario and Equations 4 to 5 are for NLOS scenario.

$$PL_{UMi-LOS} = \begin{cases} PL_1 & , 10m \leq d_{2D} \leq d'_{BP} \\ PL_2 & , d'_{BP} \leq d_{2D} \leq 5km \end{cases} \quad (1)$$

$$PL_1 = 32.4 + 21 * \log_{10}(d_{3D}) + 20 * \log_{10}(f_c) \quad (2)$$

$$PL_2 = 32.4 + 40 * \log_{10}(d_{3D}) + 20 * \log_{10}(f_c) - 9.5 * \log_{10}((d'_{BP})^2 + (h_{BS} - h_{UT})^2) \quad (3)$$

$$PL_{UMi-NLOS} = \max(PL_{UMi-LOS}, PL'_{UMi-NLOS}) \quad (4)$$

$$\text{for } 10m \leq d_{2D} \leq 5km$$

$$PL'_{UMi-NLOS} = 35.3 * \log_{10}(d_{3D}) + 22.4 + 21.3 * \log_{10}(f_c) - 0.3(h_{UT} - 1.5) \quad (5)$$

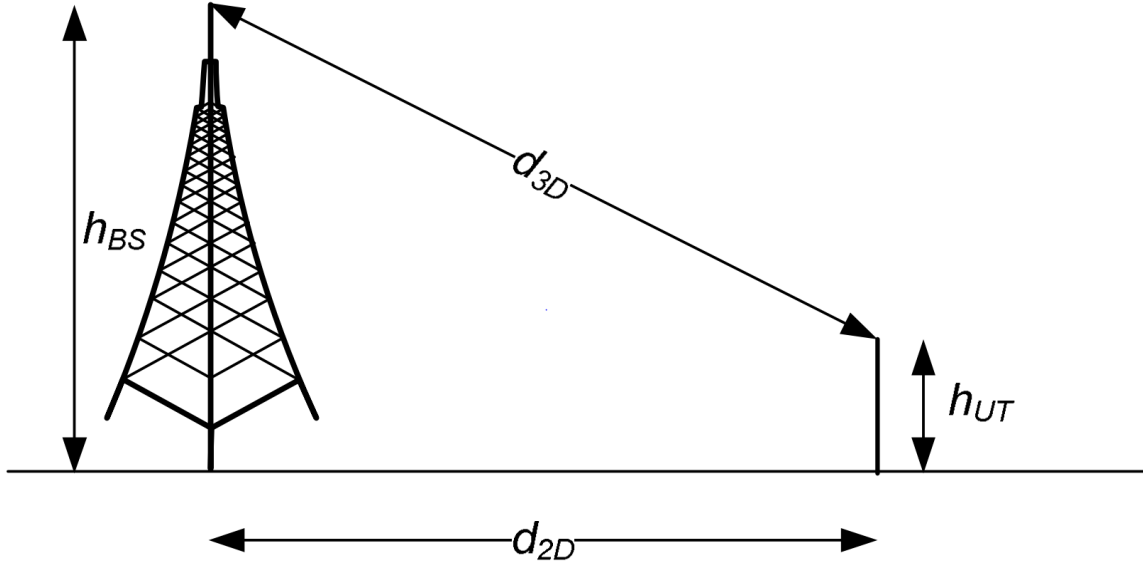


Figure 8. Definition of d_{2D} and d_{3D} for Outdoor User Terminals (UTs) (3GPP, 2022)

Where, h_{UT} is the height of the user terminal (vehicle), the range for which is dictated as $1.5\text{ m} \leq h_{UT} \leq 22.5\text{ m}$ and $h_{BS} = 10\text{ m}$ for both LOS and NLOS. The standard deviation of the shadow fading (dB) $\sigma_{SF} = 4$ for LOS and $\sigma_{SF} = 7.82$ for NLOS. f_c is the center frequency in Hz, and d'_{BP} is the breakpoint distance which has been explained in detail in TR 1389010.

The distance definitions are illustrated in Figure 8 and the standard formula for the calculation of d_{3D} is given by Equation 6. LOS probability for Umi-Street Canyon model is given by Equation 7.

$$d_{3D} = \sqrt{(d_{2D})^2 + (h_{BS} + h_{UT})^2} \quad (6)$$

$$Pr_{LOS} = \begin{cases} 1 & , d_{2D-out} \leq 18\text{ m} \\ \frac{18}{d_{2D-out}} + \exp\left(-\frac{d_{2D-out}}{36}\right)\left(1 - \frac{18}{d_{2D-out}}\right) & , 18\text{ m} < d_{2D-out} \end{cases} \quad (7)$$

2.3 Modulation and Coding Scheme (MCS)

In LTE-V2X mode 4, the MCS plays a pivotal role in shaping the transmission characteristics of communication between vehicles and RSUs. MCS dictates the modulation scheme and coding rate applied to transmitted data, influencing the efficiency and reliability of the communication link. This importance is underscored through several key aspects. Firstly, MCS selection involves trade-offs between data rate, error correction capability, and modulation complexity, crucial for achieving low latency and high reliability. Secondly, MCS adaptation facilitates dynamic responses to changing channel conditions, allowing for adjustments in scenarios of varying channel quality or interference. Thirdly, MCS directly impacts spectral efficiency, vital for optimal spectrum utilization in environments with numerous connected vehicles. Additionally, adaptive MCS contributes to collision avoidance by optimizing transmission parameters based on real-time channel conditions, ensuring minimal interference and enhancing overall system robustness. Finally, MCS is integral to resource allocation strategies in 4 LTE-V2X mode 4, ensuring the reliable and timely transmission of critical safety messages between vehicles and RSUs in dynamic vehicular environments.

LTE-V2X employs an extensive range for the values of MCSs that employ quadrature phase shift keying (QPSK) and 16-quadrature amplitude modulation (QAM) modulations, as illustrated in Table 4 of (Bazzi, et al., 2019). For the purpose of this study, specifically MCS 7 and MCS 11 with parameters as stated in (M. Garcia et. al., 2021) have been included to assess their potential impact on overall latency and PDR.

2.4 ITS Message Types

Table 2 categorizes several representative message types (i.e., as the last row) according to the “traffic families” (i.e., as the 3rd row). In particular, the ongoing SAE J3161 standardization activity (SAE, 2022) is primarily based on the end-to-end latency, namely, the packet delay budget (PDB). Discussion on the metric selection shall be revisited in Section III-D. We assign different ProSe per-packet priorities (PPPP) (3GPP ETSI TS 123303) based on the importance of a message type. This proposition is to further extension to optimization of C-V2X via assigning different communication profiles (viz., number of subchannels, modulation and coding scheme (MCS), number of retransmissions, etc.) for the packets based on packet size, velocity, and channel busy ratio (CBR). Here is elaboration of Table 2 (SAE J2745, 2020) (USDOT CV273, 2024): basic safety (BSM), emergency vehicle alert (EVA), road safety (RSM), map data (MAP), signal phase and timing (SPaT), Radio Technology Commission for Maritime Services corrections (RTCM), signal status (SSM), signal request (SRM), traveler information (TIM), and road weather (RWM), as well as even transport-layer protocols such as transmission control (TCP) and user datagram (UDP). These types of messages support a broad set of vehicle-to-vehicle (V2V) and vehicle-to-infrastructure (V2I) applications, e.g., forward collision warning, pre-crash sensing, emergency vehicle warning and signal preemption, and infrastructure-to-vehicle warning messages.

As found from the “V2V” column of Table 2, some applications operate based on the same message types, allowing numerous applications to be operated without requiring

Table 2. Mapping of Message Types to Traffic Priority Levels (SAE J2745, 2020).

Service Type	Safety Services				Mobility Services		
Traffic Direction	V2V		V2I-I2V		V2I-I2V		
Traffic Families	Critical V2V	Essential V2V	Critical V2I-I2V	Essential V2I-I2V	Transactional	Low priority	Background
Minimum PPPP	2	5	3	5	6	6	8
Minimum PDB	20 msec	100 msec	100 msec	100 msec	100 msec	100 msec	100 msec
Example Messages	BSM, EVA	BSM	RSM, MAP	Spat, RTCM	SSM, SRM	TIM, RWM	TCP, UDP

additional spectrum. However, different applications using the same message types can have vastly different spectrum needs due to differing message sizes and frequency of message transmission, so there are scenarios in which some applications using the same message types could and could not be deployed. Additionally, the available spectrum will be dependent in part on the number of vehicles within communication range and the types of applications operating in a given area. Because of this, it will likely be necessary to establish a scheme that prioritizes safety-critical applications while underrating non-safety-critical applications in such situations.

2.5 Performance Metrics

2.5.1 End-to-End Latency

The end-to-end latency is the length of maximum allowed time between the generation of a message at the transmitter's application and the reception of the message at the receiver's application (M. Garcia, et al., 2021). As this study focuses on Mode 4 of the C-V2X, the latency has been implemented as the length of time taken from the generation of a message at an application (of those listed in Table 2) at a RSU to the reception of the message by a vehicle. Here is the justification of "why" the latency is chosen as the key performance metric in this study over other metrics. First and foremost, the 3GPP 5G Service Requirement also identifies the end-to-end latency as one of the most critical performance indicators (EGPP ETSI TS 122186, 2022), based on which other requirement factors are defined. Not only that, the ongoing SAE J3161 standardization activity (SAE J3161/1A, 2022) is almost solely based on the latency, i.e., PDB.

2.5.2 Packet Delivery Rate

The calculation of the Packet Delivery Ratio (PDR) involves examining the proportion of packets that have been effectively decoded in comparison to the complete count of packets sent to all the vehicles by an RSU. A packet is classified as having been successfully received if there exists no overlap between the subchannel(s) utilized for its transmission and the subchannel(s) concurrently occupied by other transmitted packets within the same subframe. It's important to note that this assessment is conducted for each unique transmission-reception (Tx-Rx) pair, signifying the specific interaction between the sender and receiver. For instance, if an RSU disseminates an identical message to ten vehicles, this action

contributes to the packet count by ten instances. Several factors influence the Packet Delivery Ratio (PDR), including variables such as the quantity of subchannels, the interval for resource reservation, and the likelihood of resource reselection, as outlined in (A. Nabil et al., 2018). For a more practical analysis, only the vehicles within the communication range of their respective Road Side Units (RSUs) have been considered, utilizing Equation 8 to calculate the Packet Delivery Ratio (PDR).

$$PDR = \frac{\# \text{ Successfully received packets}}{\# \text{ Transmitted packets} + \# \text{ Dropped packets}} \quad (8)$$

CHAPTER 3

SYSTEM MODEL

3.1 Spatial Environment Simulator

Figure 9 illustrates an urban environment setup that was used in this paper’s simulations (SAE J3161/1A, 2022). A two-dimensional space \mathbb{R}^2 is supposed, which is defined by the dimensions of 520 m and 240 m for the north-south and the east-west axes, respectively. The RSUs are marked as green squares and the range of operation of each RSU is set to 150 m, indicated by a black circle around each RSU. There are two types of physical obstacles: trailer trucks (marked as black rectangles) and buildings (drawn as big gray squares). Moreover, we suppose *two junctions* (rather than just one) as an effort to examine any possible interference between roadside units (RSUs) on the C-V2X performance as each junction is equipped with a RSU. The connection from an RSU to a vehicle is shown by either a red or blue line: the red indicates a “blocked” connection whereas the blue means a “connected” link. The blockage can be caused by physical obstacles, viz., a building or a large 2 Fig. 1: Geometrical setup of the proposed simulator (with vehicle density of $\lambda = 1$ in the entire system space \mathbb{R}^2 trailer truck that are displayed by a large gray square and a black rectangle, respectively. The distribution of the vehicles follows a homogeneous *Poisson point process (PPP)* in . We define a general situation where a safety-critical application disseminates a message of its respective type over a C-V2X network. (See Section 2.4 for details on the message types). Unlike vehicles, locations of RSUs are fixed at each junction (T. Karunathilake et al., 2022). Furthermore, the symbols λ and θ are employed to indicate the densities of vehicles and trucks per road segment, correspondingly. A total of three road

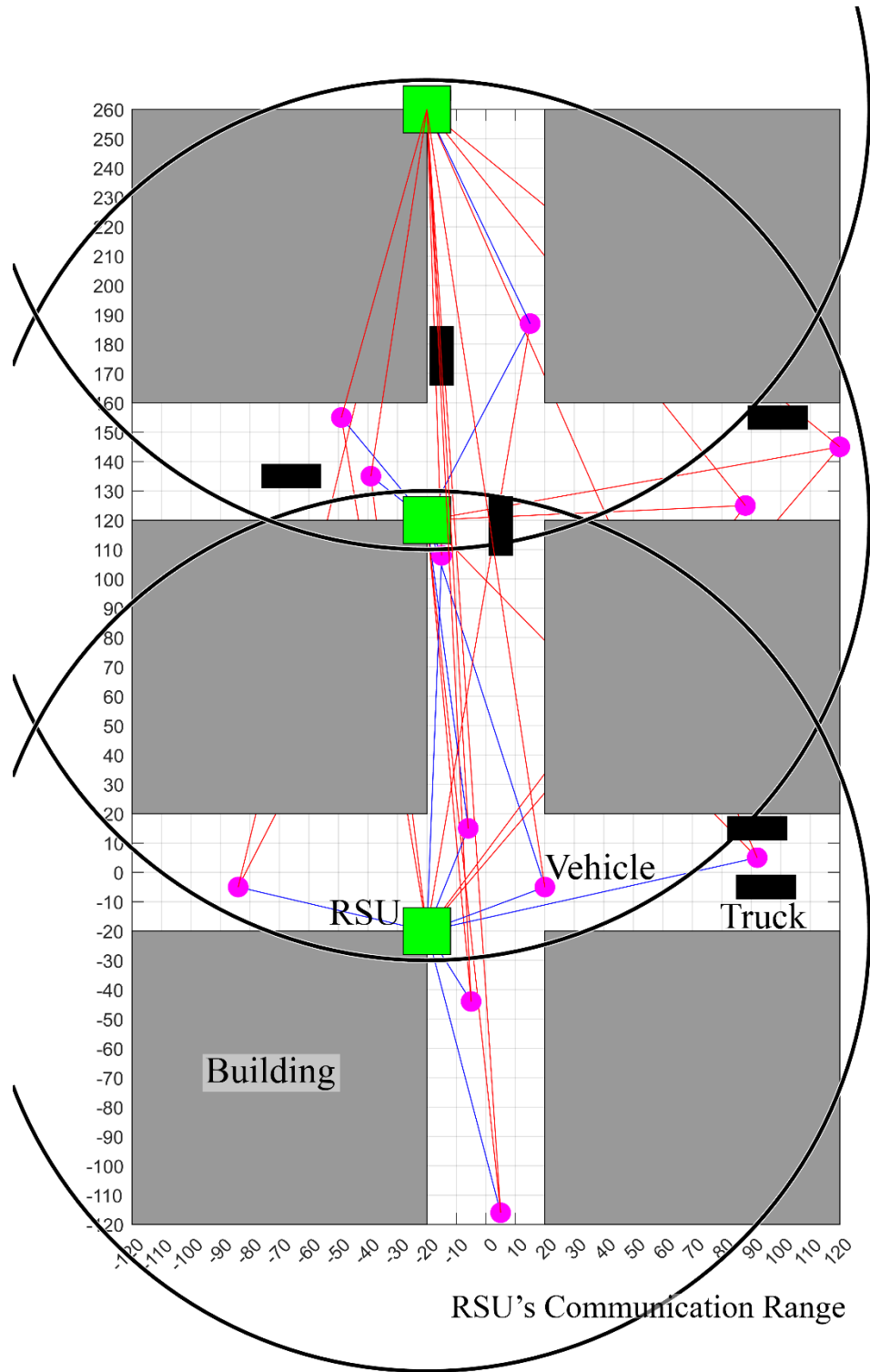


Figure 9. Geometrical Setup of the Proposed Simulator (with Vehicle Density of $\lambda = 2$ in the Entire System Space \mathbb{R}^2)

segments exist, and each of these segments comprises two directions, with each direction consisting of two lanes.

A total of six directions are considered, namely South-North, North-South, East-West 1, East-West 2, West-East 1, and West-East 2. According to the densities λ and θ , the probability of signal being blocked varies, which, in turn, influences the end-to-end latency of a message. For instance, a large λ and a large θ yield a higher level of competition for medium and an increased level of physical signal blockage, which therefore elevates the latency accordingly. It is also noteworthy that each vehicle, upon reaching the end of a road, starts over from the opposite end of the same lane. This setup is to keep the total number of vehicles constant at all times, as a means to maintain the same level of competition for the medium at any given time and thus guarantee accuracy for further stochastic analyses.

The existence of this spatial environment component adds the context of the C-V2X performance in different road/traffic settings. It can be emphasized that this component will be strengthened by adding a wider variety of road environments and traffic scenarios. The Spatial environment simulator has been developed using MATLAB where numerous parameterized variables are established, allowing for the adjustment of factors such as RSU quantity, vehicle density, truck density, vehicle speed, subchannel RBs count, inter-packet transmission intervals, and more. The sub-figures (a) and (b) in Figure 10 demonstrate the visual implications of varying lambda. The total number of vehicles appearing in the simulation is given by the value of λ entered by the user which is summarized by Equation 9.

$$\text{Total \# vehicles} = \lambda * \text{number of directions} \quad (9)$$

Where, the number of directions is set to 6 by default as there are a total of six directions.

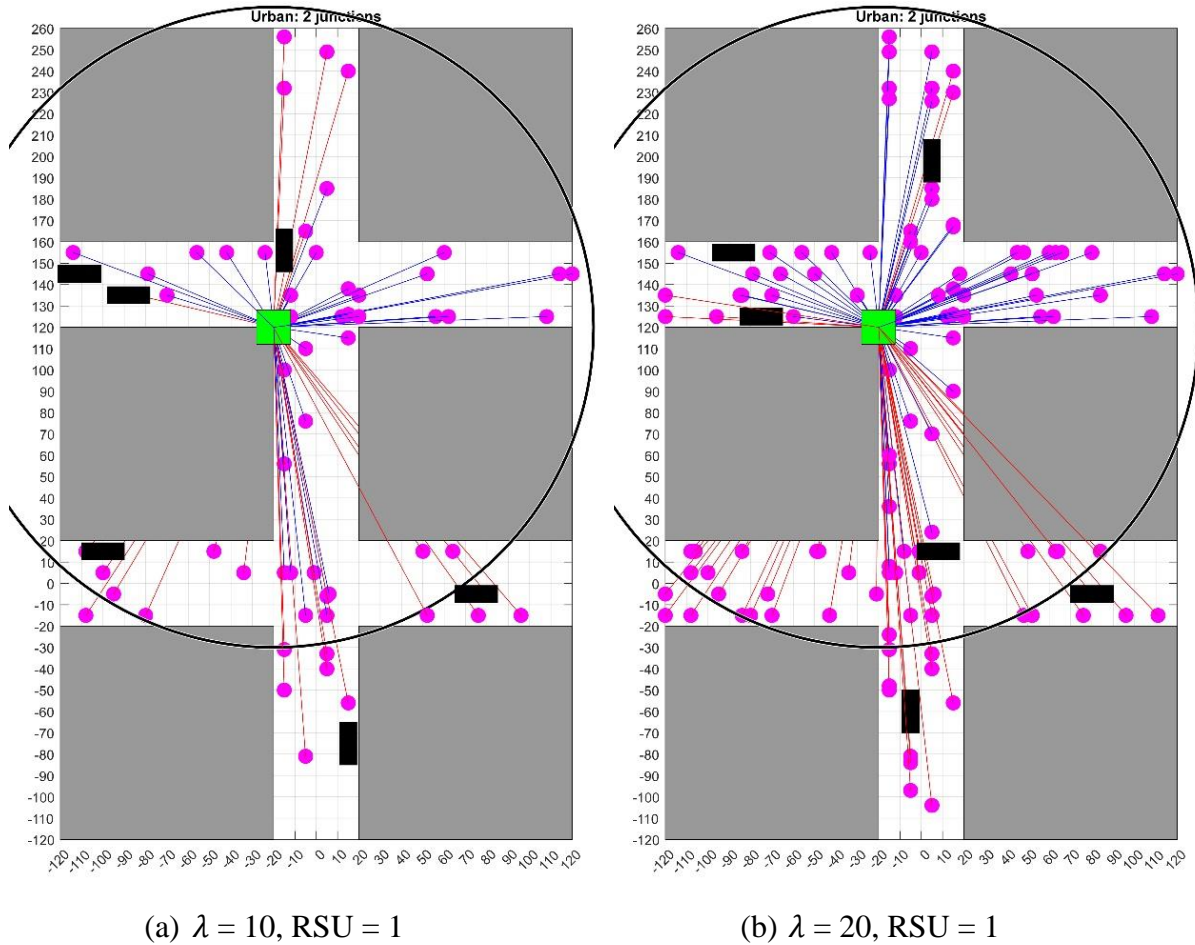


Figure 10. Number of Vehicles for $\lambda = \{10, 20\}$

The default setting for the total number of trucks, determined by the value of θ , is typically established as 1 to emulate conditions akin to those encountered in practical city road environments. Furthermore, the depiction of blocked and interconnected links, varying in response to the number of Road Side Units (RSUs), can be observed by examining the sub-figures provided in Figure 11. Upon the addition of a second RSU, notable connectivity enhancements are witnessed, particularly in the cases of the three vehicles located on the bottom side and the remaining three on the bottom-right side, which previously faced

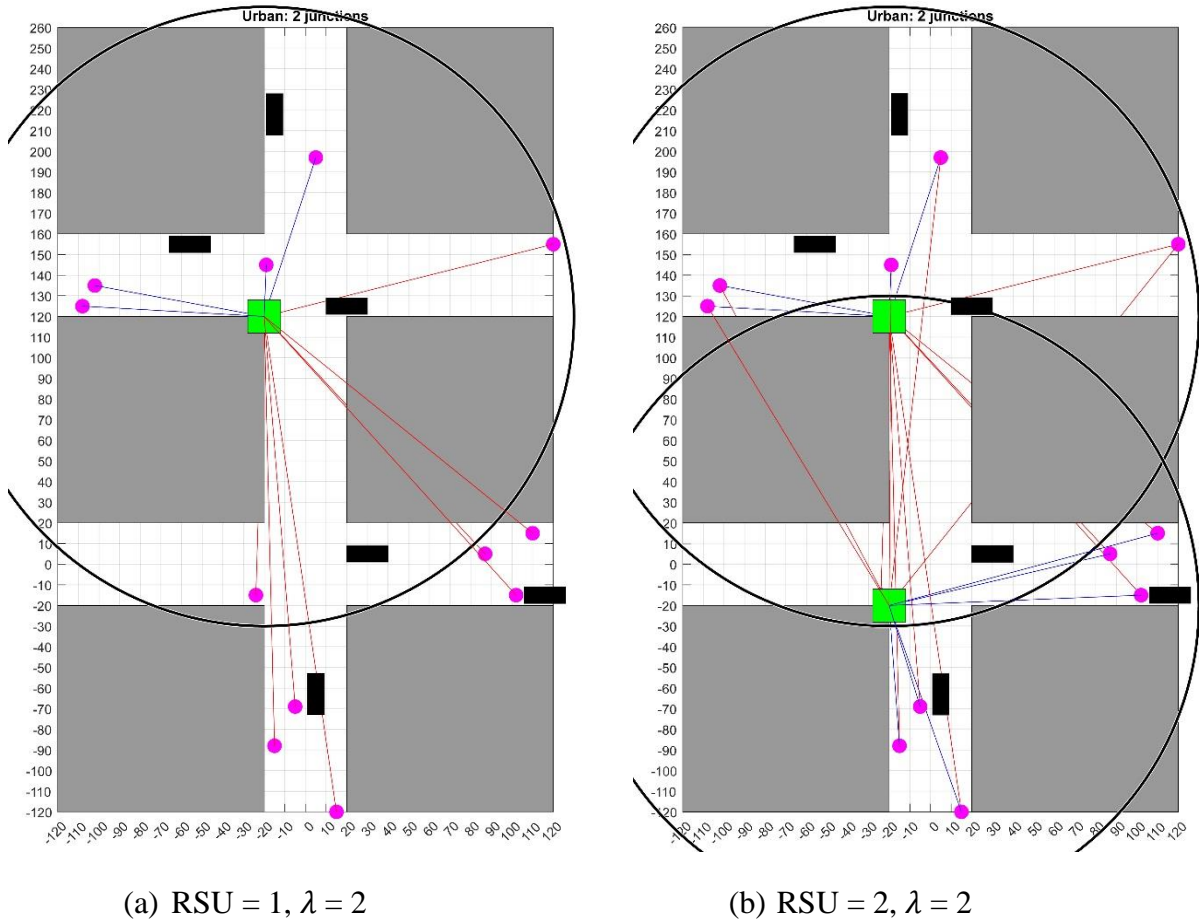


Figure 11. Connection Links with Vehicles when # RUS = {1,2} and $\lambda = 2$

obstructions when only a single RSU was present. The operational frequency bandwidth of RSUs is configured to span {10, 20} MHz. Comprehensive analyses are conducted to evaluate the performance of RSUs operating at both 10MHz and 20MHz across the subsequent data and results sections.

3.2 LTE-V2X Simulator Communication Parameters

This study adopts the 3rd Generation Partnership Project (3GPP) Release 15 Long Term Evolution (LTE)-V2X for the physical-layer (PHY) (ETSI TR 1389010, 2022) and radio resource control (RRC) functions (ETSI TS 136101). The assumption is made that Mode 4 communication takes place directly between vehicles and the Road Side Units (RSU) without going through a cellular network which is an I2V communication system. Direct communication is enabled through sidelink which is crucial for providing services like basic safety messages and traffic advisories. Mode 4 is specifically designed for low-latency and high-reliability communication, making it suitable for safety-critical applications like collision avoidance. Nonetheless, it is claimed that the versatility of the simulation framework can easily be extended to accommodate NR-V2X as well.

To elaborate on the sidelink of LTE-V2X, the simulation implements the key channels (ETSI TR 137985, 2022), namely the Physical Sidelink Control Channel (PSCCH) for transmitting physical layer sidelink control information (SCI); the Physical Sidelink Shared Channel (PSSCH) which is responsible for carrying Transport Blocks (TBs) of data; and the Physical Sidelink Broadcast Channel (PSBCH) for broadcasting basic safety messages (BSM). It is supposed that all the vehicles distributed in R2 have the same ranges of carrier sensing and communication. The possible subchannel sizes as defined by 3GPP LTE specification 36.213 (ETSI TS 136213, 2022) are {4, 5, 6, 8, 9, 10, 12, 15, 16, 18, 20, 25, 30, 48, 50 RB}, and the number of subchannels can be {1, 3, 5, 10, 15 or 20}. This paper initially assumes 50 RBs per subchannel, which matches the assumption of 10 MHz per channel and then uses varied number of RBs per subchannel to further assess the impact on latency and PDR.

3.3 Conditions for Dropping Packets

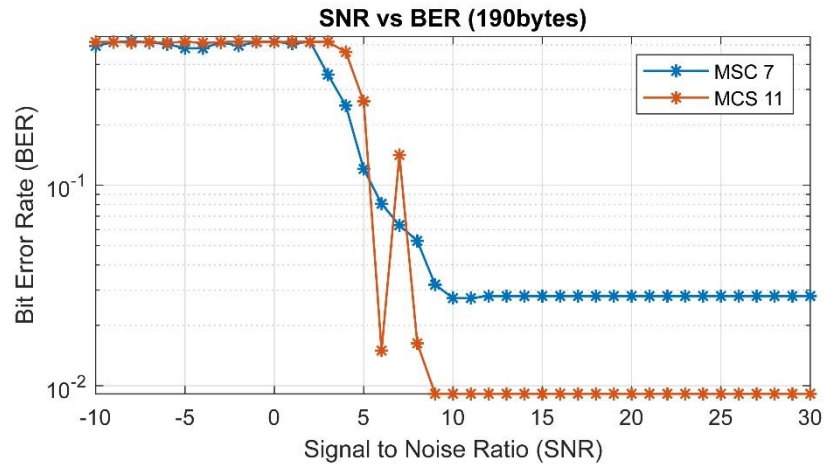
The extensive investigation delves deep into the real-world scenarios present in urban city road environments. Here, tall buildings and nearby trailer trucks can seriously weaken the strength of received signals, making it more likely for packets to get lost. Additionally, when vehicles move out of the range covered by a Road Side Unit (RSU), they lose the ability to communicate, resulting in any subsequent packets intended for them being dropped. Moreover, if the signal received becomes too weak and falls below a certain set threshold, any following packets are also dropped. This thorough study takes all these major factors contributing to packet loss into account and evaluates how they affect the overall latency and Packet Delivery Ratio (PDR) for each vehicle.

Additionally, the analysis identifies scenarios where the received signal weakens significantly, falling below predefined threshold levels. This sensitivity to signal reception heightens the risk of subsequent packets being disregarded, exacerbating challenges associated with signal degradation. This comprehensive investigation evaluates the collective impact of these factors on the overall latency and Packet Delivery Ratio (PDR) for each vehicle. The study aims to offer valuable insights into the intricate interplay among environmental conditions, signal attenuation, and data transmission efficiency, focusing on urban communication environments. The conditions defining a blocked link can be summarized in four points: a) A building obstructs the connection, b) A vehicle is beyond the RSU's range, c) A truck is positioned between a vehicle and the RSU, and d) The received signal is too faint to be detected by the receiver in the vehicles.

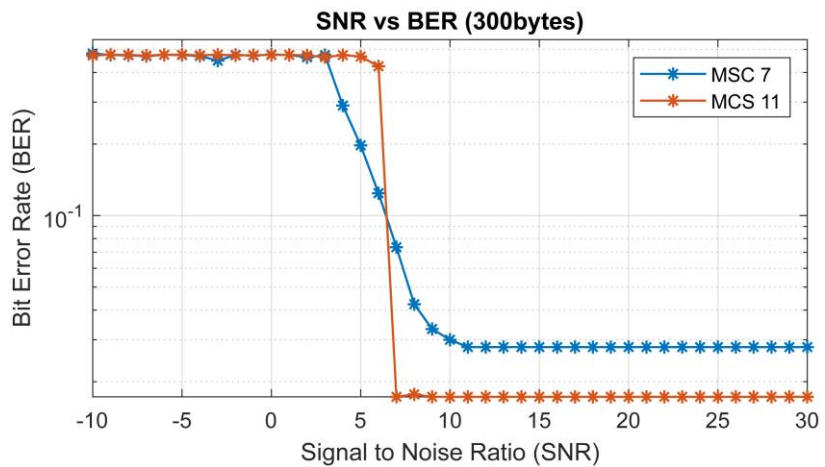
3.4 Mapping SNR and BER

In the context of LTE-V2X, the analysis of the relationship between Signal-to-Noise Ratio (SNR) and Bit Error Rate (BER) is crucial for engineers to evaluate system performance and optimize design parameters. By examining SNR versus BER, it allows one to assess how well the LTE-V2X system maintains reliable communication under varying conditions, such as interference and noise. This analysis guides the selection of modulation schemes, coding rates, and error control coding techniques to meet BER requirements while maximizing spectral efficiency and ensuring robust communication in LTE-V2X environments.

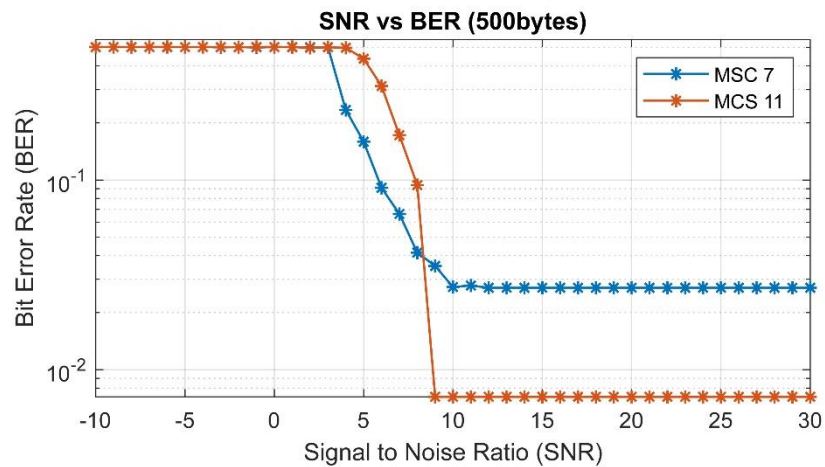
Figure 12 depicts SNR vs. BER plots illustrating the impact of message size on communication between RSUs and vehicles within their range. The message sizes are derived from SAE J3161, along with parameters such as MCS index, message types, and transmission rates. In Figure 12(a), it is observed that for smaller message sizes, BER fluctuates when the Signal-to-Interference Ratio (SIR) is below 10, whereas this fluctuation is absent for larger message sizes of 300 and 500, as shown in Figure 12(b) and 12(c) respectively. Since the study focuses on Basic Safety Message (BSM) exchange between RSUs and vehicles, a message size of 300 bytes with a BER threshold of 0.1 is considered. Research by C. Ghodhbane et al., 2022, emphasizes that interference is the main cause of packet loss at short transmitter-receiver distances, necessitating its inclusion in the study. Consequently, BER calculation with respect to the Signal-to-Interference-plus-Noise Ratio (SINR) is undertaken, with detailed procedures discussed in Section 4.3.1.



(a)



(b)



(c)

Figure 12. SNR vs BER Mapping Using MATLAB Built-In Functions with Payload (a) 190 bytes (b) 300 bytes (c) 500 bytes

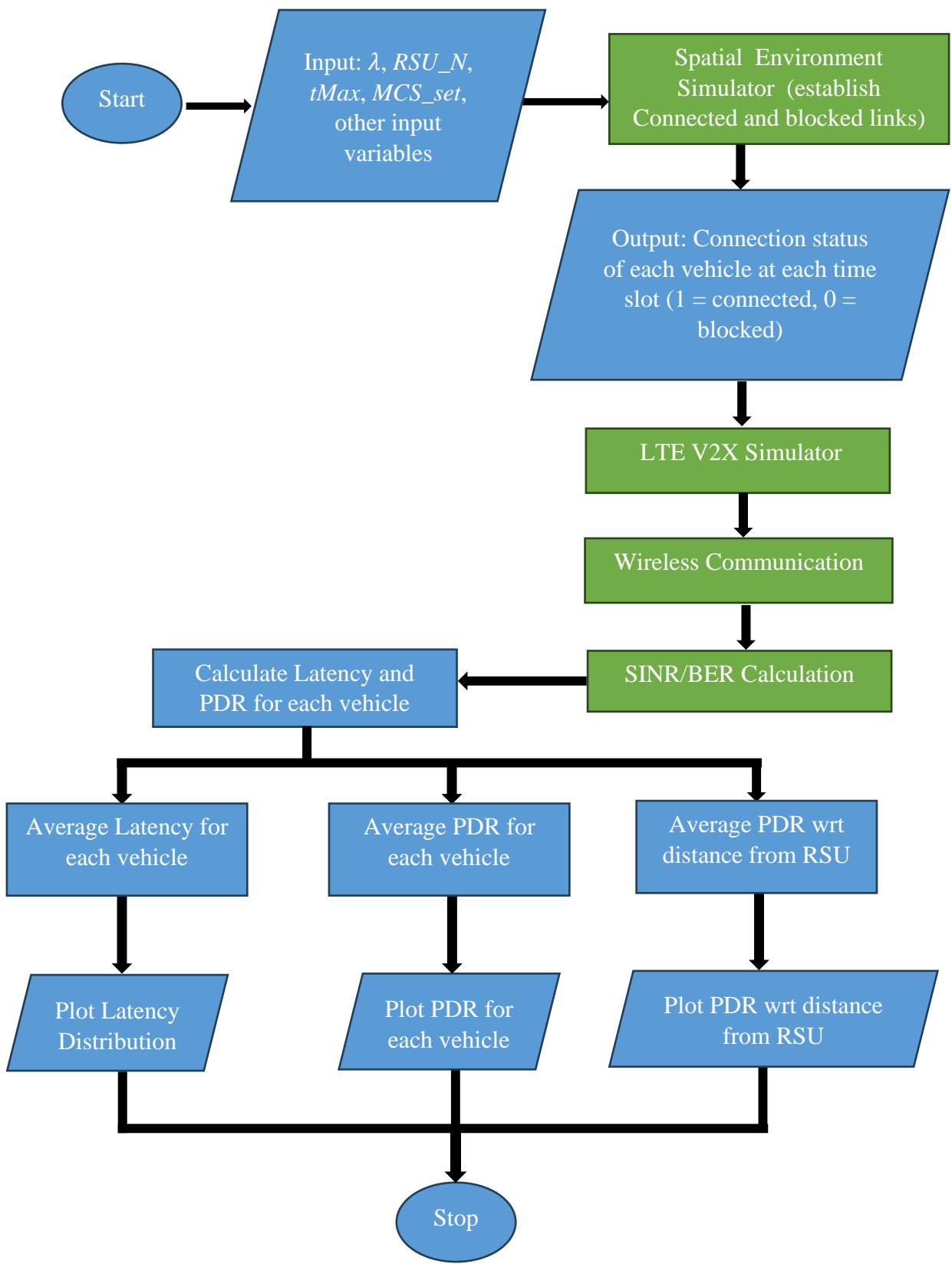


Figure 13. Basic Flowchart of the Overall Simulation

3.5 Algorithms and Flowcharts

The process flow of the simulation is outlined in the flowchart depicted in Figure 13. Each simulation begins by defining the crucial input parameters, such as vehicle density (λ), RSU count (RSU_N), maximum time slots ($tMax$), MCS index (MCS_set), and other relevant variables. These additional factors encompass truck density (θ), simulation resolution (i.e., message transmission rate), transmitted power ($power_tx$), received power threshold ($power_rx_threshold$), iteration count, vehicle and truck speeds, Resource Reservation Interval (RRI), among others. To streamline the simulation, the values of certain input variables are kept constant. Specifically, $\theta = 1$, $power_tx = 23\text{ dBm}$, $power_rx_threshold = -97.28\text{ dB}$, $vehSpeed = 12$, $truckSpeed = 18$, $RRI = 100\text{ ms}$, and so forth. The algorithm for the major processing blocks illustrated by green boxes in Figure 13 are briefly discussed below.

3.5.1 Algorithm for Establishing Connected and Blocked Lines

The function *lineSegmentIntersect()* (U. M. Erdem, 2010) takes two arguments $XY1$ and $XY2$ which contain the endpoint coordinates of the two lines and checks if these two lines intersect or not. If the function indicates an intersection, then it is a blocked link or else it must satisfy other conditions to be considered a connected line. The following algorithm has been implemented to establish the connected lines and blocked lines between the RSU and a vehicle in each timeslot.

- 1) Create a matrix, $XY1$, that contains the coordinates of the ends of each edge-line of the building.
- 2) Create a matrix, $XY2$, that contains the coordinates of the lines joining the RSU and a vehicle.

3) Run the function *lineSegmentIntersect* to check the intersection between the elements of *XY1* and *XY2*.

4) If there is an intersection, it is a blocked line, go to step 9.

else, go to step 5.

5) Calculate the distance between the RSU and the vehicle. Euclidean distance, d , between two points, RSU $(x1, y1)$ and vehicle $(x2, y2)$, in a cartesian coordinate system, is given by Equation 11.

$$d = \sqrt{(x2 - x1)^2 + (y2 - y1)^2} \quad (10)$$

6) If $d > 150$, it is a blocked line, go to step 9.

else, go to step 7.

7) Check if there is a truck in between the RSU and the vehicle using the function *lineSegmentIntersect*. If there is a truck, it is a blocked line, go to step 9.

else, go to step 8.

8) Check if the received signal strength is within the pre-defined *power_tx_threshold* ≥ -97.28 dB. If the signal strength does not satisfy the condition, it is a blocked line..

else, it is a connected line.

9) End.

3.5.2 Algorithm for LTE V2X Simulator

The LTE V2X Simulator integrates several fundamental components, among them the Semi-Persistent Scheduling (SPS) technique, the Congestion Control Mechanism (CCM), and the CBR/CR Calculations. Here, a brief outline of the SPS technique.

- **Algorithm for Semi-Persistent Scheduling:** Each vehicle follows the following steps for slot request, slot assignment, packets transmission/retransmission and finally slot release. Once the total number of packets transmitted, blocked, and received are stored for each vehicle at each time slot, the PDR and Latency values are calculated and then averaged.

- 1) Initialize the Resource Reservation Interval (RRI), number of slots, number of subchannels per slot, the range of RC counters (RC),. Also initialize the major variables, namely $packets_TXed_v$, $packets_dropped_v$, $packets_TXed_AND_RXed_v$, $Latency_v$, and PDR_v . Depending upon the MCS, the number of subchannels per slot varies.

$$\# \text{ slots} = RRI * 2$$

- 2) If a vehicle (is within the range of RSU and has a connected link) wants to connect to the RSU, the vehicle looks for available slots.

if slot is available, the RSU assigns the slot to the vehicle with RC_v .

elseif slot is full, the vehicle is placed in the FIFO queue.

- 3) The RSU transmits and retransmits a packet to the vehicle by occupying adjacent slots.

The number of re-transmissions is set to 1 (A. Hjisami et al., 2022).

$$packets_TXed_v = packets_TXed_v + 2$$

if both transmission and retransmission is complete

$Latency_v$ = time required for an RSU to transmit and retransmit a packet.

$packets_TXed_AND_RXed_v = packets_TXed_AND_RXed_v + 2$

Go to step 4.

else

$packets_dropped_v = packets_dropped_v + 2$. Go to Step 5.

4) Compare the CBR/CR limits.

if measured CBR/CR are within the limits, no packets are dropped.

else $packets_dropped_v = packets_dropped_v + 2$

5) After every RRI interval, $RC_v = RC_v - 1$. The vehicle keeps on transmitting and retransmitting subsequent packets by reserving the allocated slots until it's RC_v reaches zero. When RC_v is zero, the slot is empty, and the vehicle looks for the new slots if still connected to the RSU.

6) $PDR_v = packets_TXed_RXed_v / (packets_TXed_v + packets_dropped_v)$.

7) End

3.5.3 Algorithm for Wireless Communication

This portion of the simulator consists of major steps for wireless communication from message generation, encoding, modulation, wireless channel, demodulation, decoding, and finally BER Calculation. The basic algorithm for wireless communication has been summarized below.

- 1) Generate a 300-byte random digital signal.
- 2) Calculate the noise power using Equation 11.

$$Np = k * T_o * BW \quad (11)$$

Where, N_p is the noise power, $k = 1.38 \times 10^{-23}$ J/K is Boltzmann's constant, T_0 is the temperature in kelvin, and BW is the bandwidth.

- 3) Calculate the received power at each vehicle at each time slot from the spatial environment simulator using equation 12.

$$\text{Received Power} = \text{Transmitted Power} - \text{Pathloss} \quad (12)$$

- 4) Calculate the SINR using the SNR algorithm.
- 5) Encode the digital signal using Matlab turbo encoder function: *lteTurboEncode()*. Since the default coding rate of turbo encoder is 1/3, use *lteRateMatchTurbo()* function for rate matching to get the desired coding rate (based on MCS index).
- 6) Use *paskmod()* and *qammod()* functions for QPSK and QAM modulations respectively.
- 7) Pass the modulated signal through the AWGN channel using the *awgn()* function.
- 8) Use *paskdemod()* and *qamdemod()* functions for QPSK and QAM demodulations respectively.
- 9) Decode the received signal using Matlab turbo decoder function *lteTurboDecode()*.
- 10) Since 1 blind transmission is used, the packets are assumed to be successfully received after one transmission followed by one re-transmission, therefore, the Bit Error Rate is calculated by comparing the decoded signal with the original sent message.

3.5.4 Algorithm for SINR Calculation

Only one (Transmitter) Tx vehicle is referred to at a time and since an RSU is the (Receiver) Rx in an uplink, all the other vehicles (but the Tx vehicle), having the RSU within the Tx range, are considered for the SINR calculation. The interference can be defined by Equation 13 and the SINR can be calculated by using Equation 14.

$$I = \sum_{\{i\}} I_{\{i\}} \quad (13)$$

$$SINR = Pr / (I + Np) \quad (14)$$

Where, $I_{\{i\}} = Pt_{\{i\}} / PL_{\{i < -> RSU\}}$ and Pr is the received power by the Rx vehicle. In cases where I is large due to proximity to RSU or when a large number of vehicles are interfering Equation 14 is reduced to Equation 15 as highlighted in (C. Ghodhbane et al., 2022).

$$approx SINR = Pr / I \quad (15)$$

An example showing the calculation of SINR is as follows.

Consider a total of 6 vehicles (SN_V , NS_V , $EW1_V$, $WE1_V$, $EW2_V$, $WE2_V$), $tMax = N$, $tt = 1: tMax$, and assuming index i as Rx vehicles or RSU. Then the interference power at SN_V at $tt = 1$ (denoted by $I_{SN_V}(1)$), is the sum of interferences contributed by all the other Rx-vehicles at $tt = 1$ within the range of RSU + interference contributed by the RSU. Then from Equation 13,

$$I_{SN_V}(1) = \text{interferences due to } [NS_V(1) + EW1_V(1) + WE1_V(1) + EW2_V(1) + WE2_V(1) + RSU]$$

Where, interference due to $NS_V(1) = Pt_{\{SN_V(1)\}} / PL_{NS\{\text{calculated using the distance between } SN_V(1) \text{ and } NS_V(1)\}}$

interference due to $EW1_V(I) = P_{t_SN_V(I)} / PL_{EW1}$ {calculated using the distance between $SN_V(I)$ and $EW1_V(I)$ }

interference due to $WE1_V(I) = P_{t_SN_V(I)} / PL_{WE1}$ {calculated using the distance between $SN_V(I)$ and $WE1_V(I)$ }

interference due to $EW2_V(I) = P_{t_SN_V(I)} / PL_{EW2}$ {calculated using the distance between $SN_V(I)$ and $EW2_V(I)$ }

interference due to $WE2_V(I) = P_{t_SN_V(I)} / PL_{WE2}$ {calculated using the distance between $SN_V(I)$ and $WE2_V(I)$ }

interference due to $RSU(I) = P_{t_SN_V(I)} / PL_{RSU}$ {calculated using the distance between $SN_V(I)$ and RSU}

The co-ordinates of the RSU location are the same for all cases, the co-ordinates of $SN_V(tt)$ is constant for a particular tt , and transmitted power $P_{t_i} = 23 \text{ dBm}$ (same as that of the RSU). Then $SINR(i,tt)$ is the *signal-to-interference-plus-noise ratio* at the vehicle SN_V at tt . For $tt = I$, using Equation 15, SINR can be represented as,

$$SINR(i,1) = Pr/I_{SN_V(I)}$$

CHAPTER 4

RESULTS AND DISCUSSION

4.1 Key Parameters for Simulation

This chapter discusses the results of the simulation conducted using two different configurations, referred to as Setting 1 and Setting 2, with a focus on the corresponding outcomes concerning Latency and Packet Delivery Ratio (PDR).

4.1.1 Key Parameters for Setting 1

The primary aim of this configuration is to determine whether the decreased 30 MHz bandwidth adequately fulfills the latency demands associated with each message type outlined in Table 2. In this configuration, each RSU functions within a 10 MHz bandwidth, while employing a Resource Reservation Interval (RRI) of 50 milliseconds, thereby accommodating 50 time slots within each RRI period. The variability in the number of RSUs ranges from 1 to 3, and the number of subchannels per slot adjusts according to the activation status of the Congestion Control Mechanism (CCM): 1 subchannel when CCM is inactive and 2 subchannels when CCM is activated. The transmission frequency is set at 20 Hz, and the Range of Re-selection Counters (RC) is established within the range of 10 to 30, adhering to the specifications outlined in earlier sections. The RC value is randomly selected within this range, with a decrement of one occurring after each transmission cycle.

Table 3 summarizes the key parameters that were used in our C-V2X simulation. Notice from the table that we assume 50 RBs per subchannel, which occupies $180 \text{ kHz/RB} \times 50 \text{ RBs/subchannel} \approx 9 \text{ MHz}$ and thus takes up most of an entire 10-MHz channel considering 1.25 MHz of a guard band [25]. The vehicle density is another noteworthy

parameter: $\lambda = \{10, 20, 30\}$ vehicles per direction equal $\{60, 120, 180\}$ vehicles in \mathbb{R}^2 , which in turn indicate $\{24, 12, 6\}$ m of minimum and $\{38, 19, 9\}$ m of maximum inter-vehicle distance. As such, we intend that the $\lambda = \{10, 20, 30\}$ vehicles per direction represent the $\{\text{low, medium, high}\}$ vehicle density, respectively. It should be noted that this Setting does not employ the impact of MCS, and blind retransmission is disabled.

Table 3. Key Parameters for Simulation with Setting 1.

Parameter	Value
Inter-broadcast interval	50 msec
Bandwidth per channel	10 MHz
Number of RBs per subchannel	50 for CCM = OFF, 25 for CCM = ON
Number of Subchannels/msg	1 when CCM = 0, 2 when CCM = 1
Payload length	40 bytes
Vehicle density	$\{10, 20, 30\}$ vehicles/direction
Number of RSUs	$\{1, 2, 3\}$
Tx Power	23 dBm
Rx Sensitivity	-180.5 dBm
Message Tx Rate	20 Hz

4.1.2 Key Parameters for Setting 2

A single RSU is considered with a bandwidth of 20 MHz (which corresponds to 5905 – 5923 MHz) that is divided into two subchannels with 50 RBs per subchannel for MCS 7 and 7 subchannels with 14 RBs per subchannel for MCS 11. Two MCS index 7 and

11 are considered for this configuration because MCS 7 represents a trend for QPSK modulation and MCS 11 represents the trend for QAM modulation, however, it should be noted that the simulator can operate in any of the 21 MCS indices listed in Table 4 of the study in (A. Bazzi et al., 2019). Each vehicle is allowed for one transmission followed by one blind retransmission. Vehicle densities considered in this configuration are: $\lambda = \{5, 10, 15, 20\}$, which is equivalent to $\{30, 60, 90, 120\}$ vehicles in \mathbb{R}^2 and a mean vehicle speed is set to 12 m/sec. The key parameters for this configuration have been highlighted in Table 4.

Table 4. Key Parameters for Simulation with Setting 2.

Parameter	Value
Inter-broadcast interval	100 msec
Bandwidth per channel	20 MHz
Number of RBs per subchannel	20 for MCS 7, 12 for MCS 11
Number of Subchannels/msg	5 for MCS 7, 8 for MCS 11
MCS indices	{7,11}
Modulation	{QPSK, QAM}
Coding rate	{0.57, 0.41}
Payload length	300 bytes
Vehicle density	{5, 10, 15, 20} vehicles/direction
Number of RSUs	1
Tx Power	23 dBm
Rx Sensitivity	-97.28 dBm
Message Tx Rate	10 Hz

4.2 RSU-to-Vehicle Latency

4.2.1 RSU-to-Vehicle Latency with Setting 1

Initially, the Congestion Control Mechanism (CCM) is deactivated in this scenario to assess the latency distribution under high vehicle density conditions. Subsequently, its activation allows examination of how it aids in resource management by equitably distributing resources among the connected vehicles.

Varying λ and RSU with CCM Disabled

The subfigures presented in Figures 14-16 offer a detailed visualization of the probability density function (pdf) representing RSU-to-vehicle latency, denoted as x in milliseconds (msec), across various RSU counts, specifically $RUS=\{1,2,3\}$. Alongside a constant vehicle density λ , set to 10 in Figure 14, 20 in Figure 15, and 30 in Figure 16, each pdf is meticulously compared against a red vertical line indicating the 20 msec latency requirement as delineated in Table 2. This thorough comparison not only elucidates the percentage of vehicles in R^2 capable of supporting diverse message types and applications but also reveals a distinct trend. Through vertical analysis within each subset of Figures 14-15, it becomes evident that a greater number of RSUs, each occupying a full 10-MHz channel, leads to a reduction in latency, thereby diminishing the likelihood of latency exceeding the specified requirement. However, as vehicle density increases, as seen in 14(a), 15(a), and 16(a), latencies surpass the 20 msec threshold. It is noteworthy that in scenarios with low vehicle density, as illustrated in Figure 14(a), the presence of a solitary RSU ensures adequate support for applications necessitating a 20 msec latency, whereas for higher vehicle densities, a single RSU is apparently insufficient to meet the latency requirement for critical messages.

.Despite the efficacy of increasing RSU count in mitigating latency below the 20 msec threshold for low and medium vehicle density scenarios, an overcrowded channel becomes evident when vehicle density is exceedingly high, as demonstrated in Figure 10 (b). Consequently, the augmentation of RSUs alone proves inadequate in lowering overall latency below the specified threshold. In such contexts, the implementation of a Congestion Control Mechanism (CCM) becomes imperative. In the context of Setting 1, aligned with our primary objective of evaluating latency impact across varied vehicle density and RSU count, we opt for a simplified version of the congestion control mechanism delineated in section 4.2 of ETSI TS 103574. Within the current simulation framework, the increase in vehicle density, indicative of a higher number of vehicles, prompts a halving of Resource Blocks (RBs) per subchannel, ensuring a fairer distribution of resources among vehicles within range. Nevertheless, such adjustments may potentially compromise the resilience and reliability of transmitted messages, necessitating a delicate balance between resource allocation and message dependability. Thus, while addressing the challenges posed by high vehicle density, it becomes essential to optimize resource utilization without compromising the integrity of communication protocols or the reliability of transmitted data.

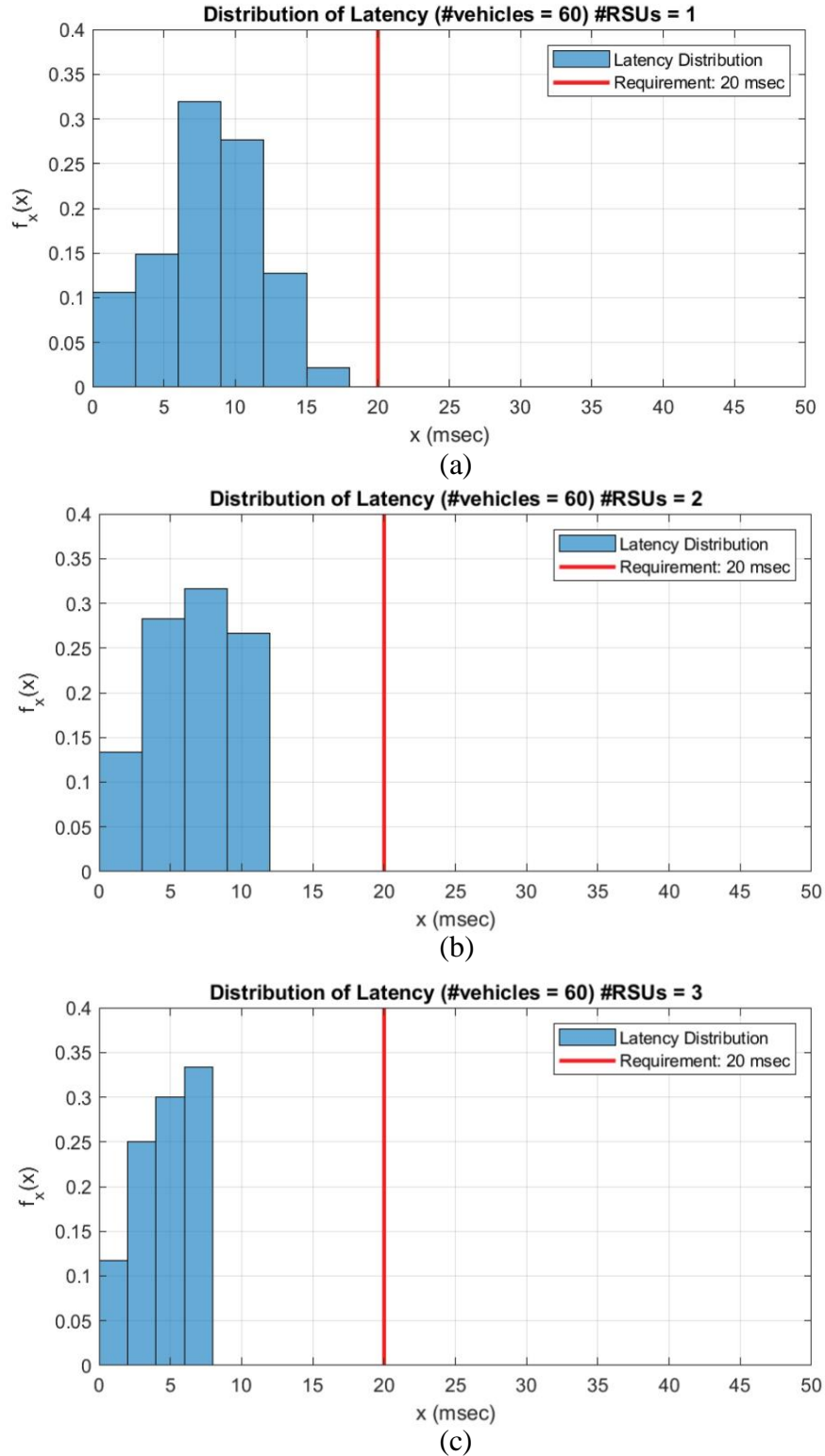


Figure 14. Distribution of RSU-to-Vehicle Latency and Traffic Density ($\lambda = 10$) Compared to Latency Requirements of 20 msec as Red Vertical Line. (a) RSU = 1 (b) RSU = 2 (c) RSU = 3

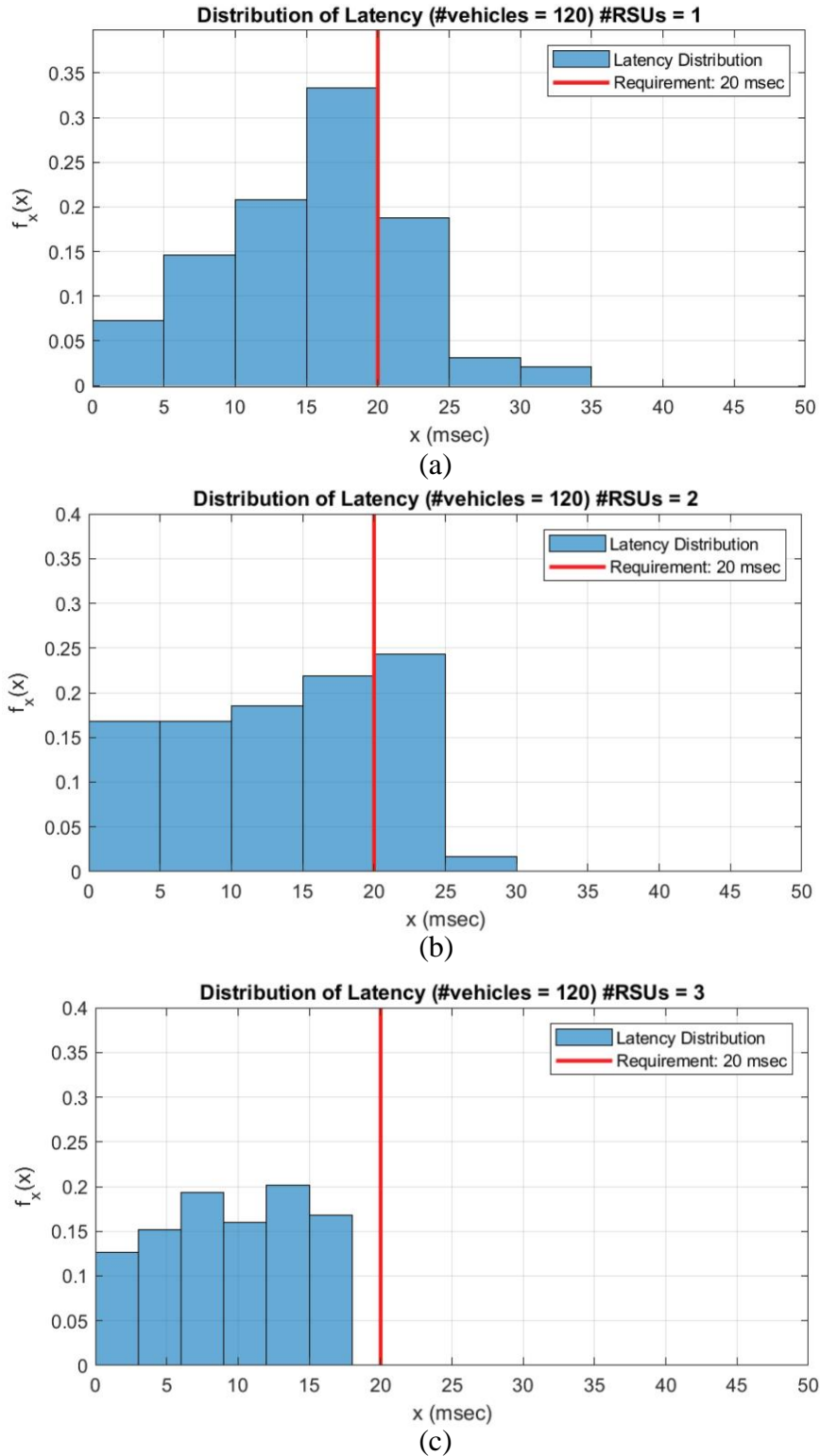


Figure 15. Distribution of RSU-to-Vehicle Latency and Traffic Density ($\lambda = 20$) Compared to Latency Requirements of 20 msec as Red Vertical Line. (a) RSU = 1 (b) RSU = 2 (c) RSU = 3

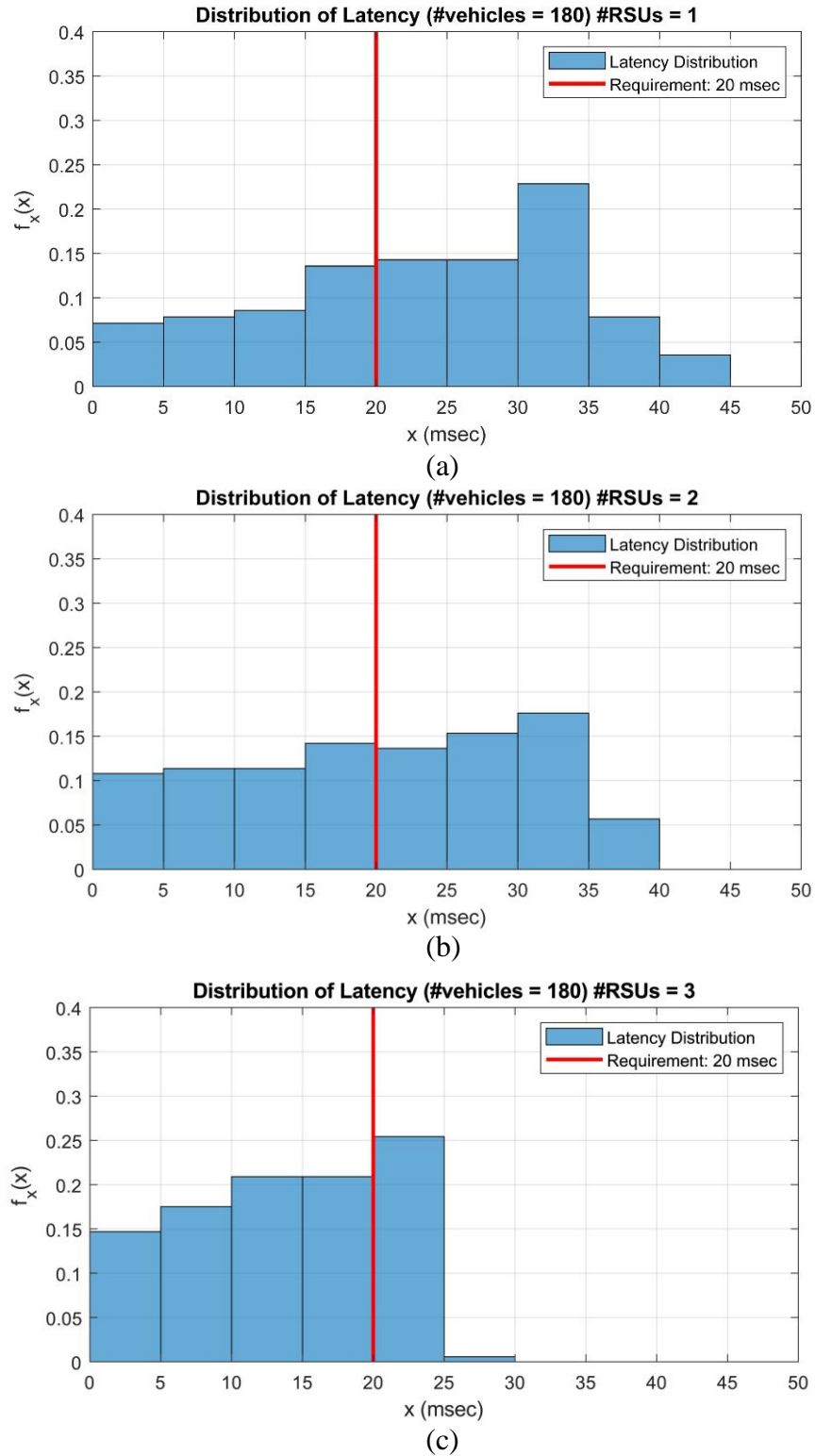


Figure 16. Distribution of RSU-to-Vehicle Latency and Traffic Density ($\lambda = 30$) Compared to Latency Requirements of 20 msec as Red Vertical Line. (a) RSU = 1 (b) RSU = 2 (c) RSU = 3

Varying λ and RSU with CCM Enabled

This section delves into the pivotal role played by the Congestion Control Mechanism (CCM) in efficiently managing available resources, particularly when faced with scenarios characterized by a significant influx of vehicles seeking connection to the Road Side Unit (RSU). In situations of low vehicle density, even with just a single RSU, applications with a latency requirement of 20 msec are adequately supported. However, as the vehicle density increases, latencies exceed the 20 msec threshold; nevertheless, an increase in the RSU count results in an overall reduction in latency below 20 msec. The results presented in Figures 14 to 16 are derived from simulations conducted without the implementation of a Congestion Control Mechanism, resulting in elevated latency values, especially in scenarios with higher vehicle density. To assess the most challenging conditions, a heightened vehicle density ($\lambda = 30$, equivalent to 180 vehicles) was considered with a single RSU. In the absence of a Congestion Control Mechanism, as depicted in Fig. 16(a), latency far exceeds the 20 msec benchmark. However, upon integrating a Congestion Control Mechanism, latency for the majority of vehicles decreases below 20 msec, as shown in Fig. 17(a).

Intriguingly, the incorporation of both a congestion control mechanism and two RSUs leads to an additional reduction in latency, as highlighted in Fig. 17(b). A comparison between Figure 16(a) and Figure 17(a) reveals a significant reduction in overall latency due to the implementation of CCM, decreasing from a maximum of 45 msec to a maximum of 24 msec. Despite the addition of an extra RSU, as depicted in Figure 16(b), resulting in a 5 msec latency reduction, nearly half of the vehicles still experience latency exceeding the 20 msec threshold. Even with the integration of three RSUs utilizing the full 30 MHz

bandwidth, not all vehicles meet the 20 msec latency requirement, as illustrated in Figure 16(c). However, with the activation of CCM and the presence of two RSUs, nearly all vehicles exhibit latencies falling within the threshold, as shown in Figure 17(b). Finally, by employing three RSUs and CCM, compliance with the 20 msec latency requirement for all message types can be ensured, even in scenarios of exceptionally high vehicle density. Moreover, these findings emphasize that the requirement of a 20 msec latency, even in scenarios of high vehicle density, can be met through the use of three RSUs, utilizing the full 30 MHz bandwidth, alongside the implementation of CCM, as illustrated in Figure 17(c).

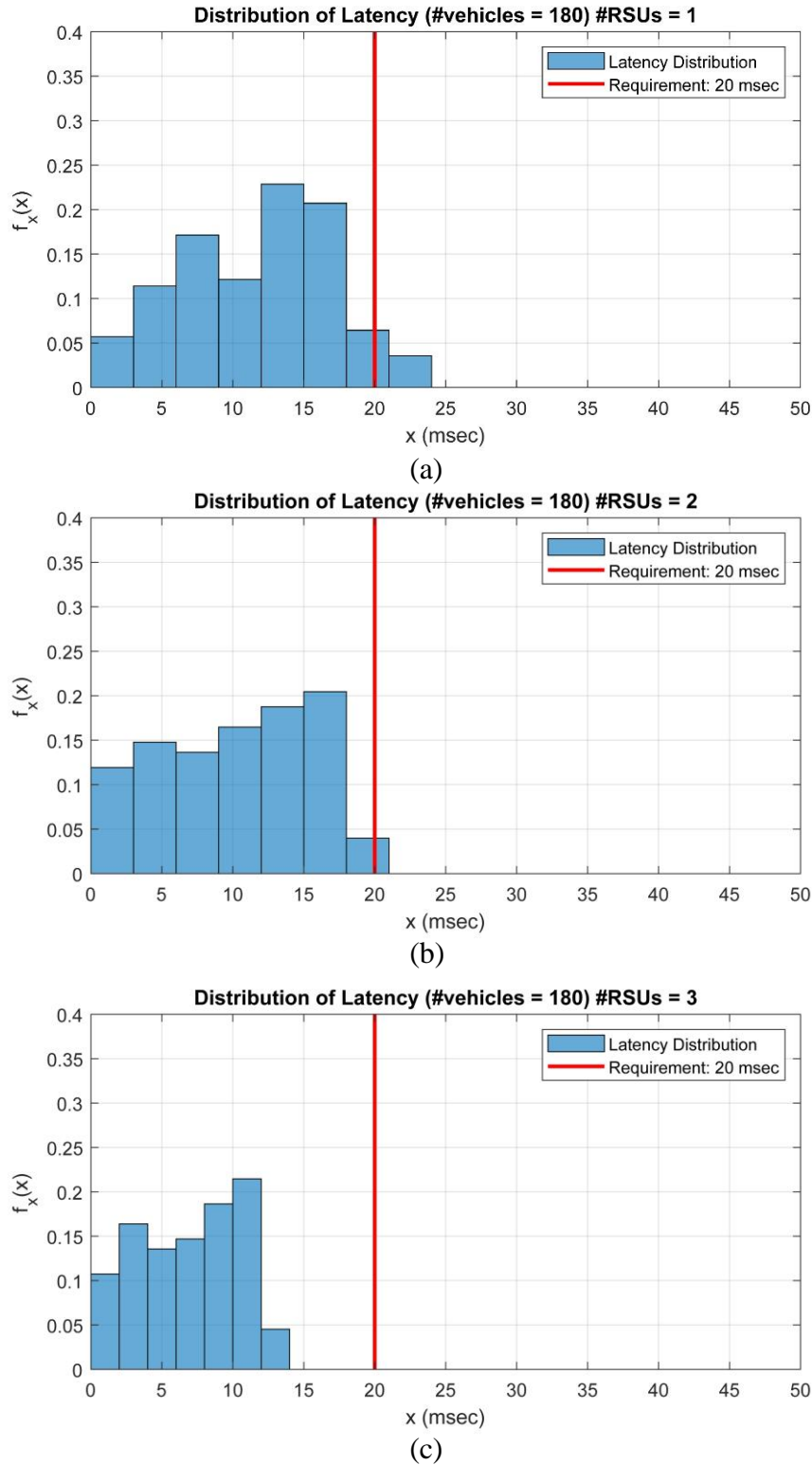


Figure 17. Distribution of RSU-to-Vehicle Latency (Congestion Control Mechanism Enabled) and Traffic Density ($\lambda = 30$), Compared to Latency Requirements of 20 msec as Red Vertical Line. (a) RSU = 1 (b) RSU = 2 (c) RSU = 3

Varying Speed of Vehicles with CCM Disabled

This series of findings delves into the nuanced impact of varying mean vehicle speeds on overall latency within the LTE-V2X communication framework. With the λ value set at 15, translating to a total of 90 vehicles in \mathbb{R}^2 , the default mean vehicle speed remains steady at 12 m/s, with associated results depicted in Figure 18 (b). Furthermore, the latency distributions corresponding to halved vehicle speeds (6 m/s) and doubled vehicle speeds (24 m/s) are illustrated in Figure 18 (a) and (c), respectively. Upon meticulous observation of the subfigures, it becomes evident that subtle alterations in mean vehicle speed yield only marginal adjustments in the overall latency distribution among vehicles.

Upon closer examination of the histogram distributions, an observable trend emerges: an increase in mean vehicle speed marginally widens the overall latency distribution towards the higher end, while a decrease in mean vehicle speed slightly compresses the overall latency plots. However, in the broader context, these slight variations in latency do not exert significant effects. Given that traffic speeds in urban environments typically adhere to limits well within the 24 m/s threshold, LTE-mode 4 communication experiences minimal disruptions due to speed variations. However, in high-speed highway scenarios, the situation differs markedly due to factors like Doppler shift and the effects of handovers, which may compromise latency. In practical scenarios, additional factors such as handover effects, modulation and coding schemes, and signal quality degradation at higher speeds further contribute to latency increases under elevated speed conditions.

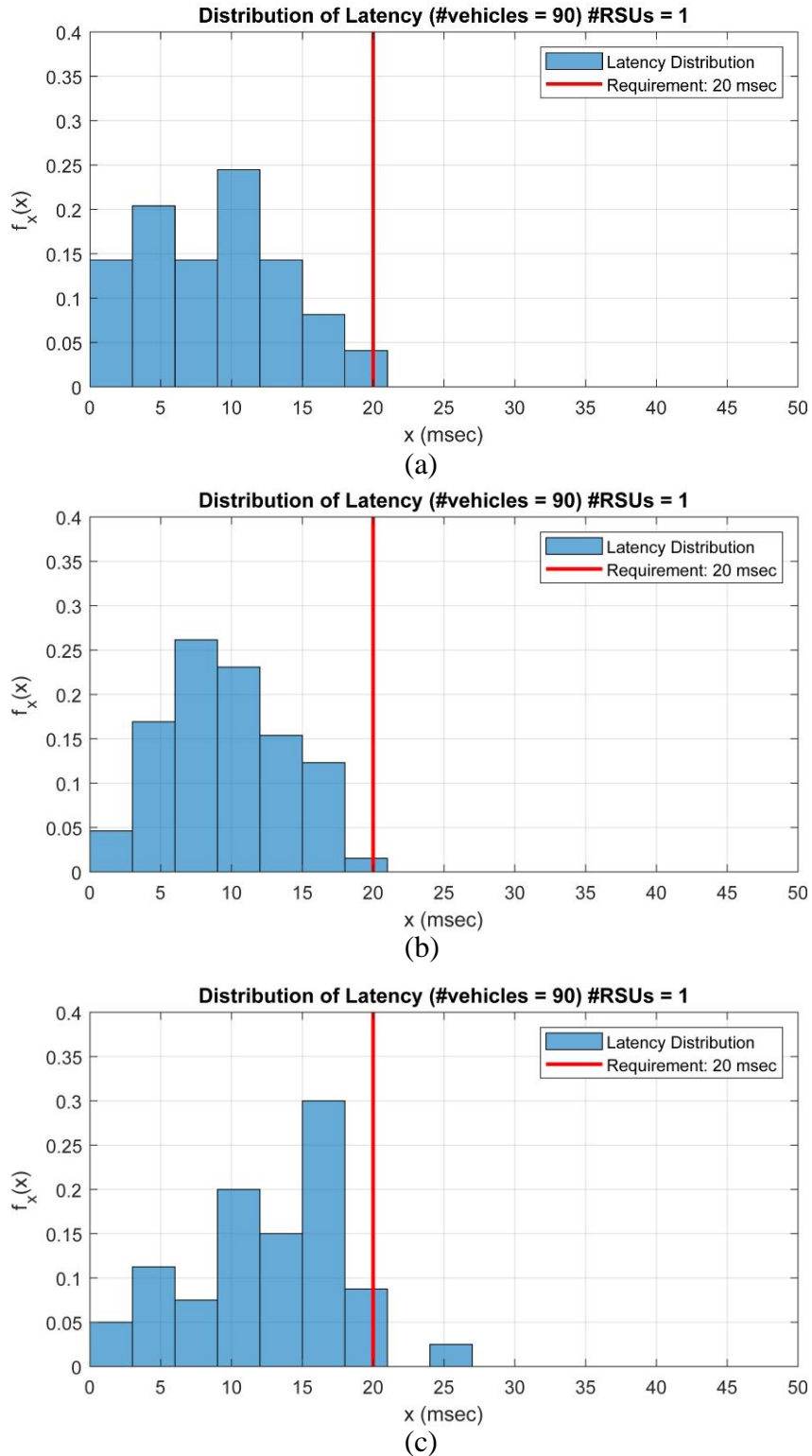
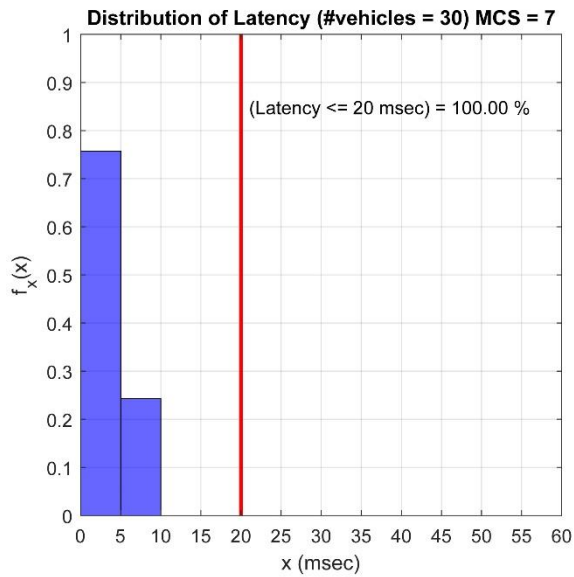


Figure 18. Distribution of RSU-to-Vehicle Latency (Congestion Control Mechanism Disabled) and Traffic Density ($\lambda = 15$) Compared to Latency Requirements of 20 msec as Red Vertical Line. The Mean Vehicle Speed is Set to (a) 6 m/s, (b) 12 m/s, and (c) 24 m/s

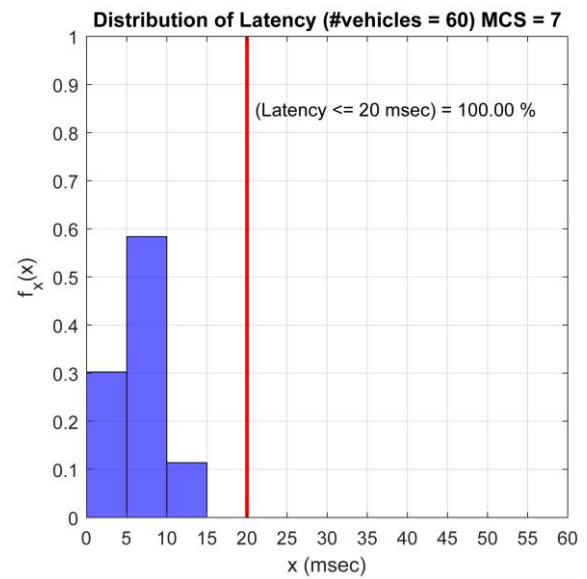
4.2.2 *RSU-to-Vehicle Latency with Setting 2*

Within this series of results, a comprehensive exploration delves into the influence of Modulation and Coding Scheme (MCS) on both latency and, more notably, Packet Delivery Ratio (PDR). Unlike in Setting 1, where the RSU count remains variable, here it's fixed at 1, operating within a 20 MHz bandwidth. These findings, associated with varying lambda values {5, 10, 15, 20}—equating to traffic densities {30, 60, 90, 120}—and MCS indices {7, 11}, are meticulously illustrated in Figure 19 and Figure 20. Mirroring the structure in Setting 1, both figures depict the probability density function $f_X(x)$ of RSU-to-vehicle latency x in milliseconds, with a red vertical reference line indicating the minimum PDB requirement outlined in Table 2.

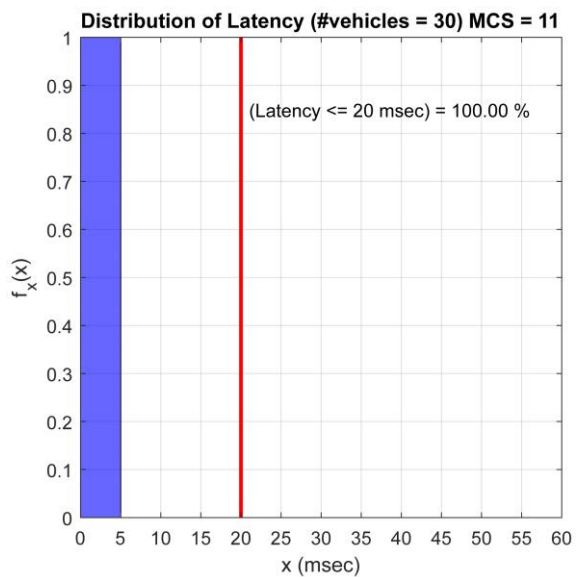
A horizontal comparison across the first and second rows of both figures (namely, Figs. 19a, 19b, 20a, 20b, and Figs. 19c, 19d, 20c, 20d) reveals a clear pattern: as vehicle density increases while maintaining a fixed MCS, overall latencies experience a corresponding increase. This surge in vehicle density gives rise to heightened competition among vehicles, resulting in intermittent wait times for other vehicles to successfully receive transmitted signals. Furthermore, vertical inspection within each column consistently reveals that the utilization of MCS 11 consistently leads to lower latencies compared to MCS 7 across the respective vehicle densities. This divergence comes from the fact that a higher MCS index affords a greater coding rate and modulation order, enabling more efficient information transmission per symbol and consequently higher data rates. Consequently, the possibility of reducing the size of Resource Blocks (RBs) per subchannel for each Transport Block (TB) becomes viable, thereby subdividing the available bandwidth into more subchannels capable of accommodating a larger quantity of vehicles.



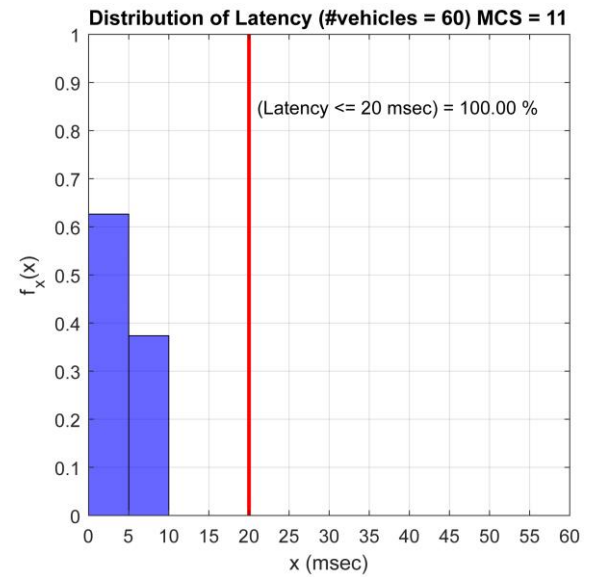
(a) MCS 7 and 30 vehicles



(b) MCS 7 and 60 vehicles

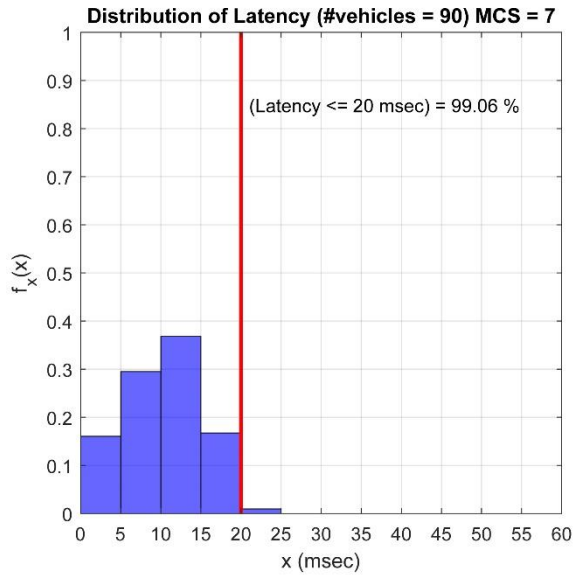


(c) MCS 11 and 30 vehicles

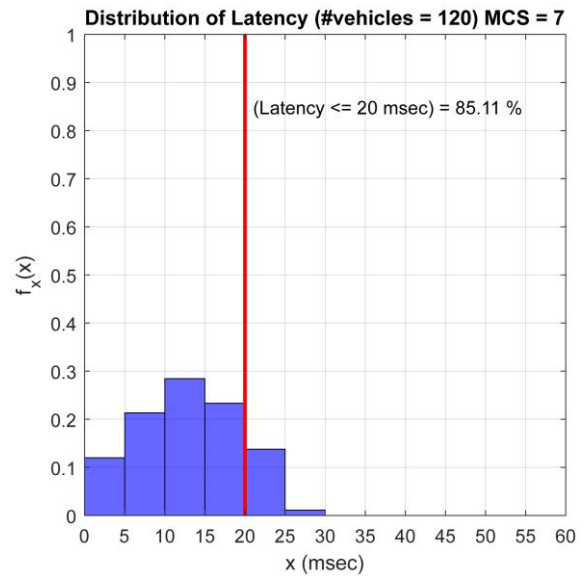


(d) MCS 11 and 60 vehicles

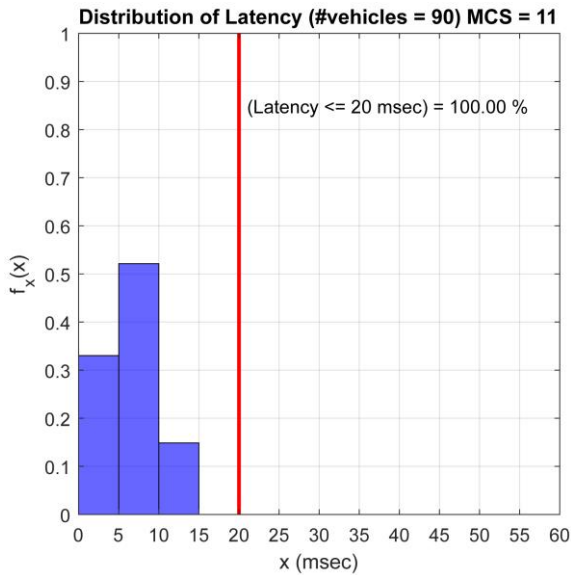
Figure 19. Distribution of Latency According to MCS Index = {7, 11} (Compared Column-Wise) and Traffic Density = {30, 60} (Compared Row-Wise) Compared to Latency Requirement of 20 msec as Red Vertical Line



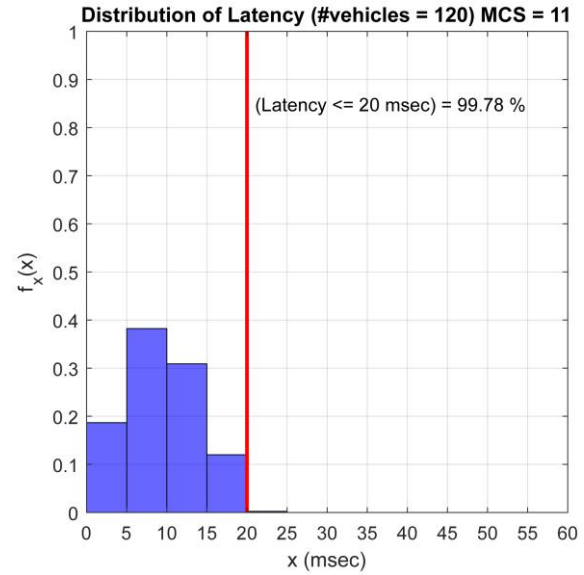
(a) MCS 7 and 90 vehicles



(b) MCS 7 and 120 vehicles



(c) MCS 11 and 90 vehicles



(d) MCS 11 and 120 vehicles

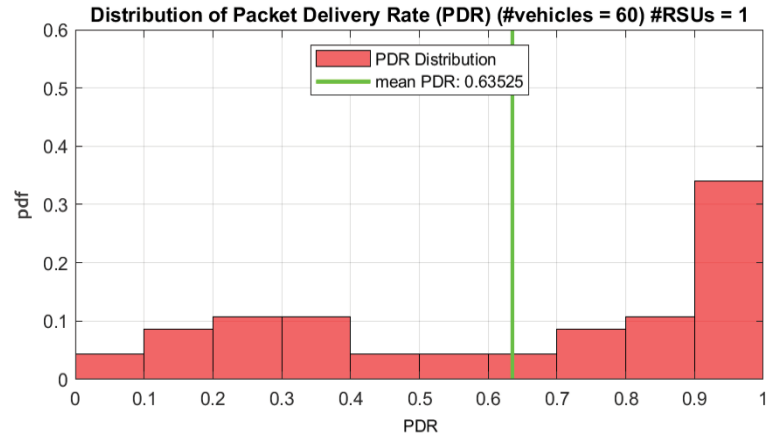
Figure 20. Distribution of Latency According to MCS Index = {7, 11} (Compared Column-Wise) and Traffic Density = {90, 120} (Compared Row-Wise) Compared to Latency Requirement of 20 msec as Red Vertical Line

4.3 Packet Delivery Rate (PDR)

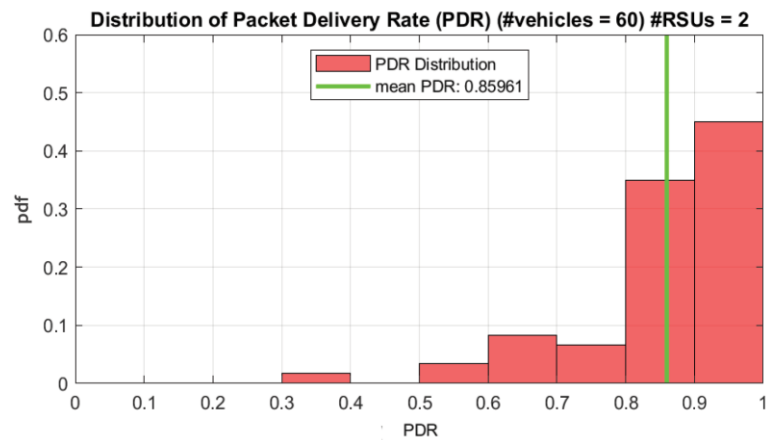
4.3.1 PDR Distribution with Setting 1

The average distribution of Packet Delivery Rate (PDR) for RSU configurations {1, 2, 3} is depicted in subfigures (a), (b), and (c) within Figure 21 and Figure 22, respectively. Vertical comparison within each set of subfigures in both Figure 21 and 22 underscores that an increased number of RSUs correlates with heightened PDR and enhanced reliability. This augmentation in RSUs expands the available resource pool, thereby influencing the observed outcomes. Additionally, when comparing Figure 21(a) with Figure 22(a), Figure 21(b) with Figure 22(b), and Figure 21(c) with 22(c), a noticeable trend emerges where higher vehicle density corresponds to reduced PDR. Remarkably, the mean PDR for all vehicles within a specific configuration is denoted by the green vertical line, signaling an increase in PDR with the addition of RSUs and a decrease with heightened traffic density.

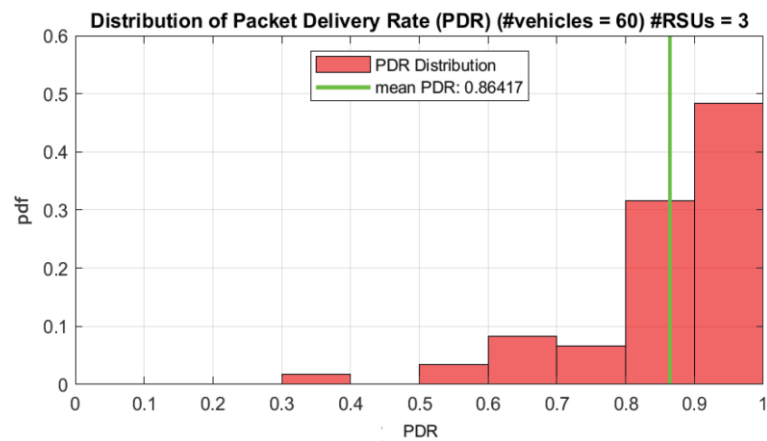
While enabling Congestion Control Mechanism (CCM) significantly improved latency, the distributions of PDR remained relatively consistent regardless of whether CCM was enabled or disabled. This consistency arises from the focus of Setting 1, where the complete implementation of Modulation and Coding Scheme (MCS) was not prioritized. The primary aim of the study was to examine Latency and PDR concerning their feasibility with reduced frequency bandwidth, rather than overall Quality of Service in V2X communication. Nevertheless, future iterations of the simulator will incorporate improvements in this aspect as part of ongoing enhancement efforts.



(a)

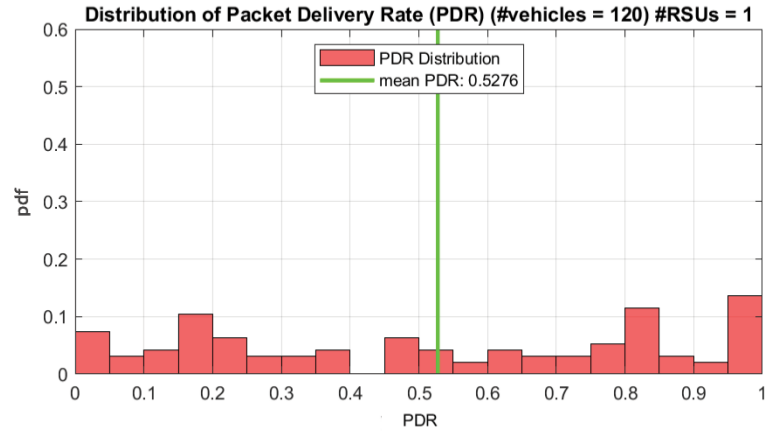


(b)

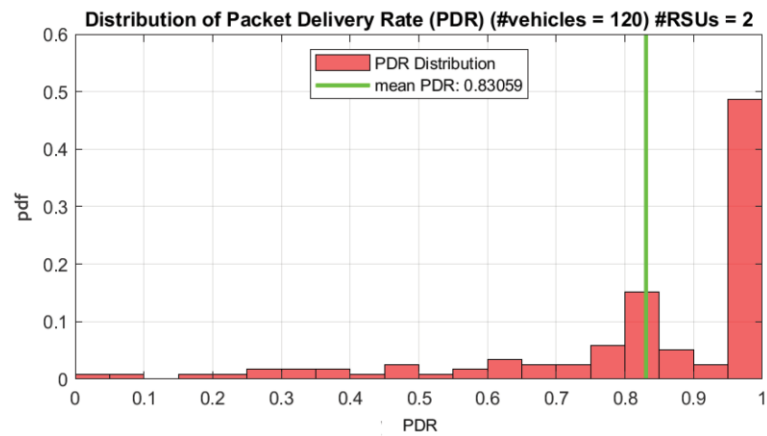


(c)

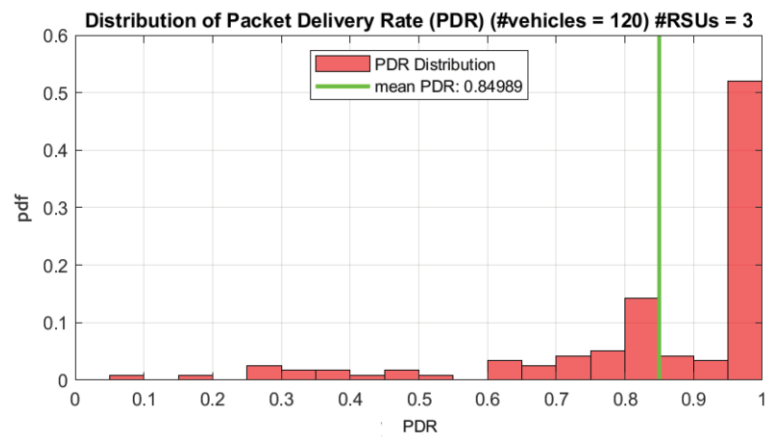
Figure 21. Distribution Packet Delivery Rate (PDR) According to Number of RSUs and Traffic Density ($\lambda = 10$) Showing the Mean PDR Values (Indicated by the Green Vertical Line)



(a)



(b)



(c)

Figure 22. Distribution Packet Delivery Rate (PDR) According to Number of RSUs and Traffic Density ($\lambda = 20$) Showing the Mean PDR Values (Indicated by the Green Vertical Line)

4.3.2 PDR Distribution with Setting 2

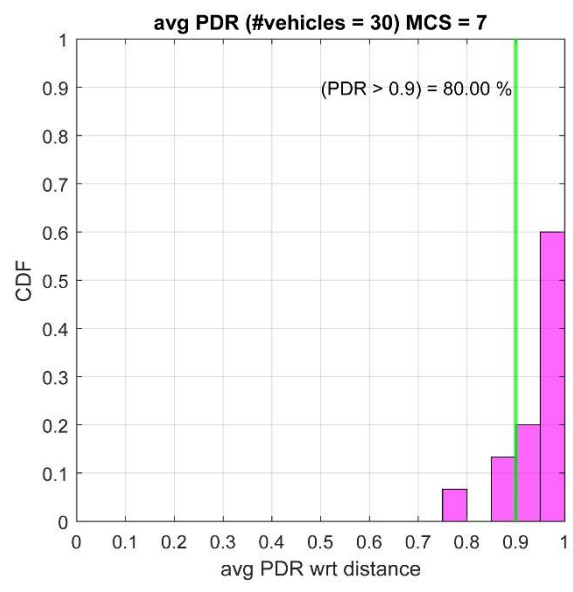
The PDR distributions achieved by altering the number of RSUs closely resemble those of setting 1. As the primary focus in this setting is to examine PDR distributions for different MCS settings, the outcomes related to varied λ and MCS {7, 11} are presented in the subsequent section.

Varied λ and MCS

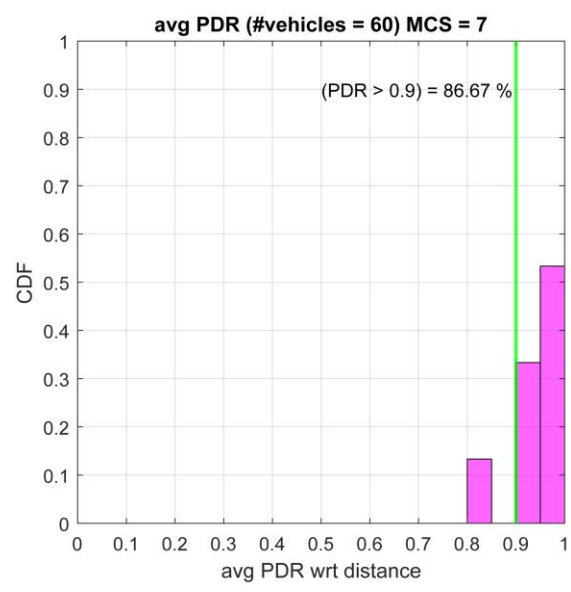
The PDR results, depicted through the cumulative distribution function (CDF) for PDR, are visualized in the subfigures of Figure 23 and Figure 24. These results are correlated with specific MCS values, {7, 11}, and traffic densities, $\lambda = \{10, 15, 20\}$, corresponding to traffic densities of {30, 60, 90, 120}, respectively. The vertical green lines serve as pivotal references, delineating thresholds beyond which vehicles achieve a PDR exceeding 0.9. Notably, in scenarios characterized by low traffic density (i.e., 30), over 90% of total vehicles exhibit a PDR surpassing 0.9 for both MCSs, 7 and 11, as depicted in Figure 23(a) and Figure 23(c). However, with an increase in vehicle density, the proportion of vehicles exceeding the 0.9 PDR threshold diminishes below 90%. It's imperative to highlight that for critical message types such as BSM and EVA, a PDR approaching 1 is highly desirable. Particularly in scenarios with medium to high traffic densities (i.e., 60, 90, 120), the utilization of MCS 7 yields a higher number of vehicles achieving a PDR exceeding 0.9 compared to MCS 11.

The latency distribution plots offer clear insights, indicating that in scenarios involving both MCS 7 and MCS 11, a 20 MHz channel accommodates all message types with a minimum latency of 100 milliseconds. A notable trend emerges wherein the adoption of MCS 11 consistently maintains latency distribution below the 20-millisecond threshold

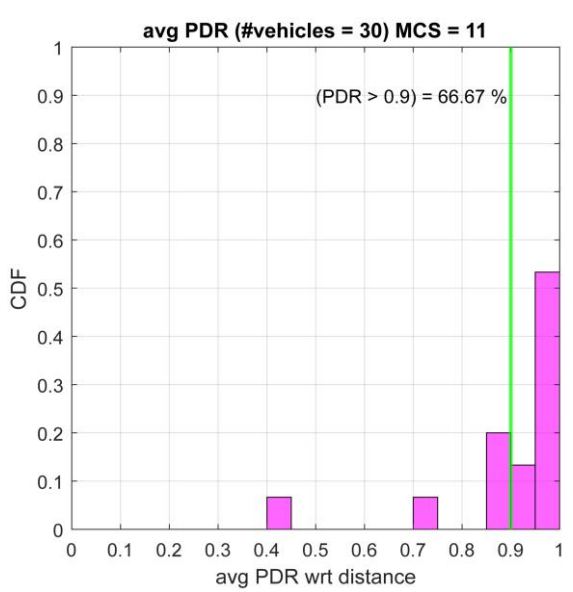
for all traffic densities $\lambda = \{5, 10, 15, 20\}$. Conversely, when MCS 7 is employed, the latency distribution exceeds the 20-millisecond threshold with increasing traffic density. However, the advantage of lower latency with MCS 11 comes with a trade-off—a reduction in overall PDR. Specifically, while higher MCS indices are expected to yield increased data rates, they also introduce heightened susceptibility to errors influenced by factors such as distance from the RSU, interference, and obstacles. Notably, significant obstacles like large trailer trucks and buildings play a crucial role in reducing the overall PDR as the MCS index transitions from 7 to 11. Despite variations in PDR values, it's noteworthy that more than 75% of total vehicles exhibit a PDR above 0.9 across all vehicle densities and both MCS indices. This observation underscores a confident assertion that a 20 MHz channel adequately supports the majority of critical messages and nearly all other essential message types outlined in Table 1.



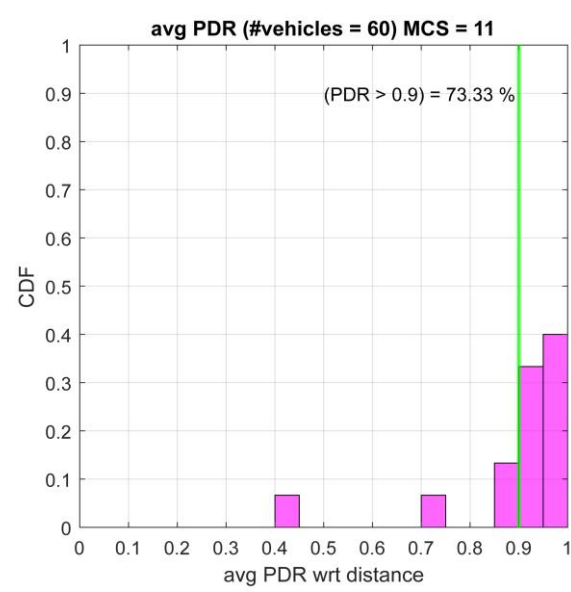
(a) MCS 7 and 30 vehicles



(b) MCS 7 and 60 vehicles

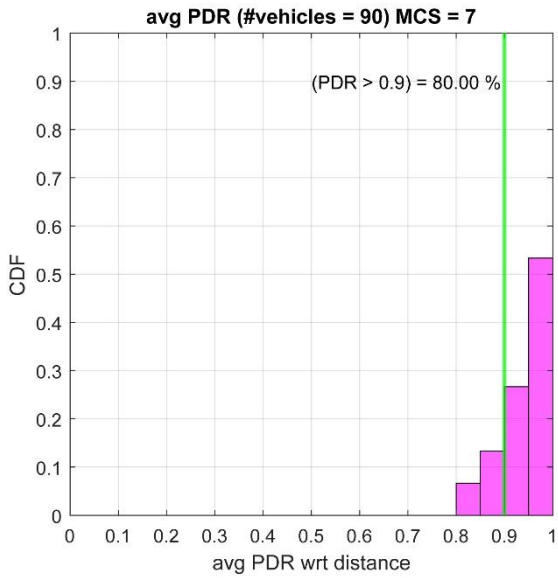


(c) MCS 11 and 30 vehicles

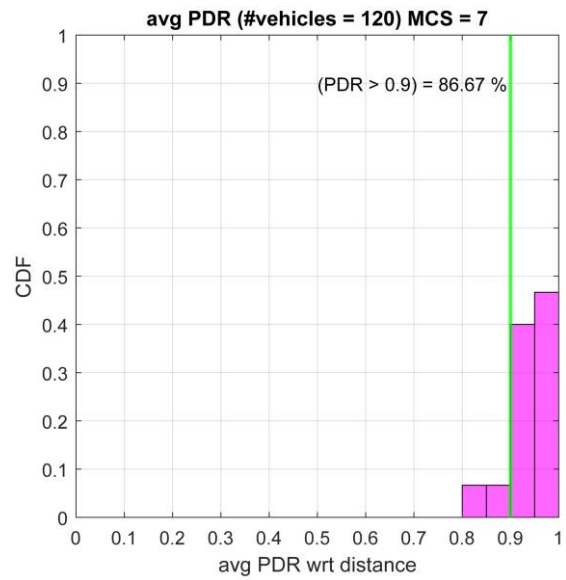


(d) MCS 11 and 60 vehicles

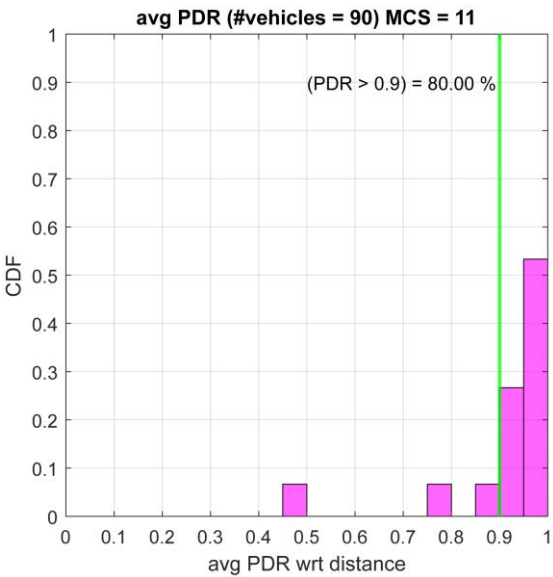
Figure 23. Distribution of PDR According to MCS Index = {7, 11} (Compared Column-Wise) and Traffic Density = {30, 60} (Compared Row-Wise)



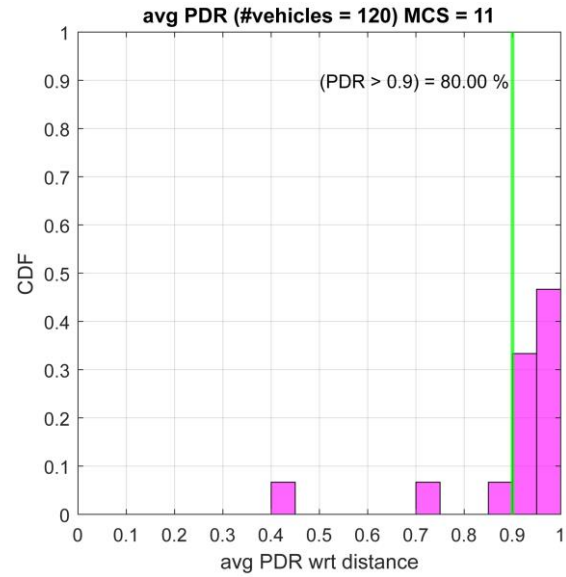
(b) MCS 7 and 90 vehicles



(c) MCS 7 and 120 vehicles



(d) MCS 11 and 90 vehicles



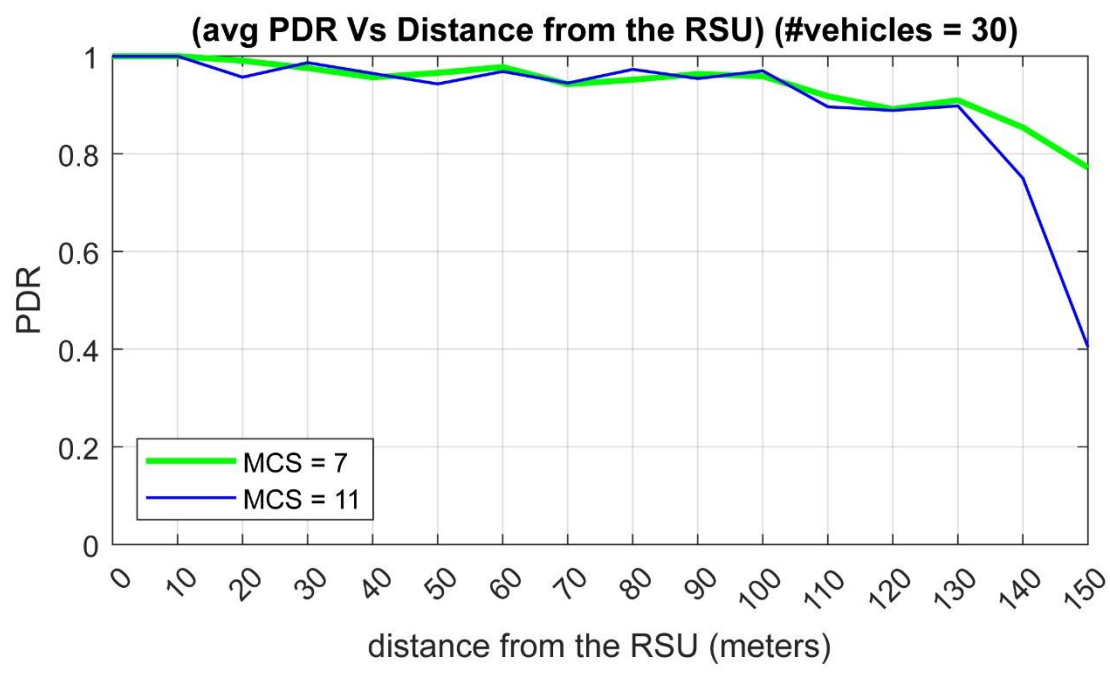
(e) MCS 11 and 120 vehicles

Figure 24. Distribution of PDR According to MCS Index = {7, 11} (Compared Column-Wise) and Traffic Density = {90, 120} (Compared Row-Wise)

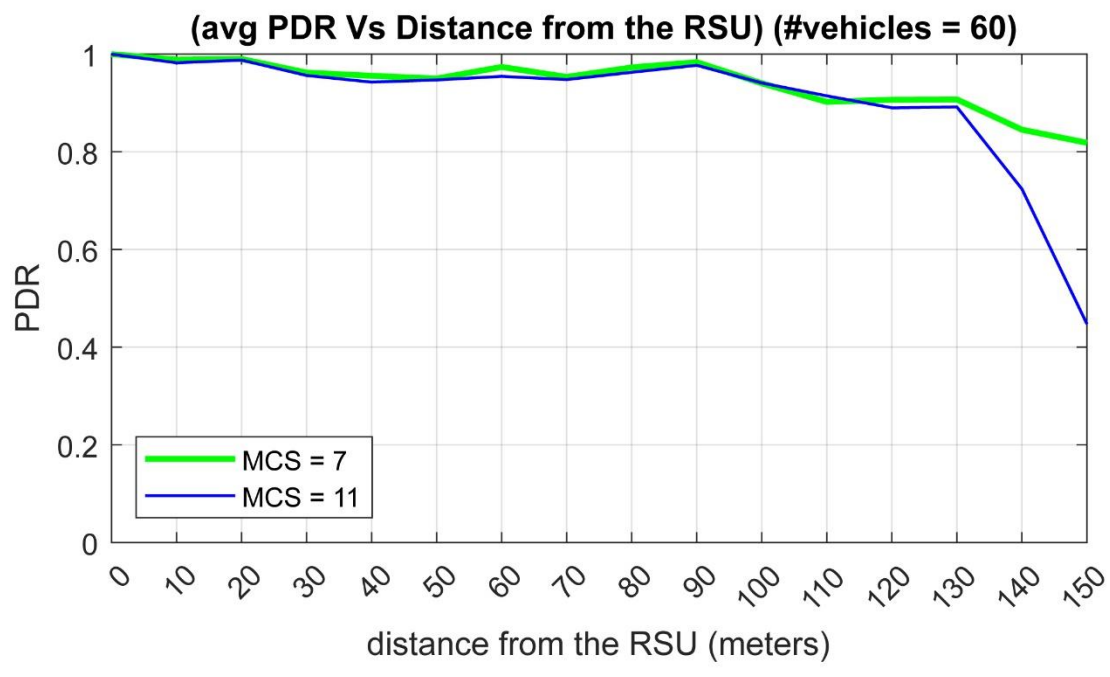
4.4 PDR vs Distance from RSU

The average values of PDR with respect to distance from the RSU are illustrated in the subfigures of Figure 25 and 26. The PDR are averaged over every 10 m distance from the RSU and are plotted. As before, a single RSU, operating at 20 MHz (utilizing Setting 2), with number of vehicles = {30, 60, 90, 120} are considered. It can be observed that irrespective of the vehicle density a constant trend appears with respect to MCS 7 and MCS 11. In all cases of Figure 25 and 26, the PDR plots for MCS 7 and MCS 11 are comparable until the distance of 130 m from the RSU, however, exceeding that distance MCS 11 seem to be dropping down which is also illustrated by the bins at PDR = 0.4 and 0.7 in the subfigures (d) and (e) of Figure 22, 23, and 24.

The performance superiority of MCS 7 over MCS 11 can be ascribed to several key factors. Firstly, MCS 7 typically operates at a lower modulation scheme and coding rate compared to MCS 11. This characteristic results in a transmission that is inherently more robust, especially in environments characterized by high levels of noise or interference. Additionally, MCS 7 often demands a lower Signal-to-Noise Ratio (SNR) for successful decoding when compared to MCS 11, thereby enhancing its resilience to external factors. Furthermore, the lower modulation complexity of MCS 7 enables it to offer a wider coverage area and better penetration through obstacles. In particular, in a city road environment dominated by tall buildings and large trailer trucks, MCS 7 tends to establish more reliable communication links compared to MCS 11. This advantage underscores the importance of selecting the appropriate modulation and coding scheme tailored to the specific challenges and requirements of the communication environment.



(a) for $\lambda = 5$



(b) for $\lambda = 10$

Figure 25. PDR Variation for $\lambda = \{5, 10\}$ with Respect to Distance from the RSU where Green Plots Indicate MCS 7 and Blue Plots Indicate MCS 11

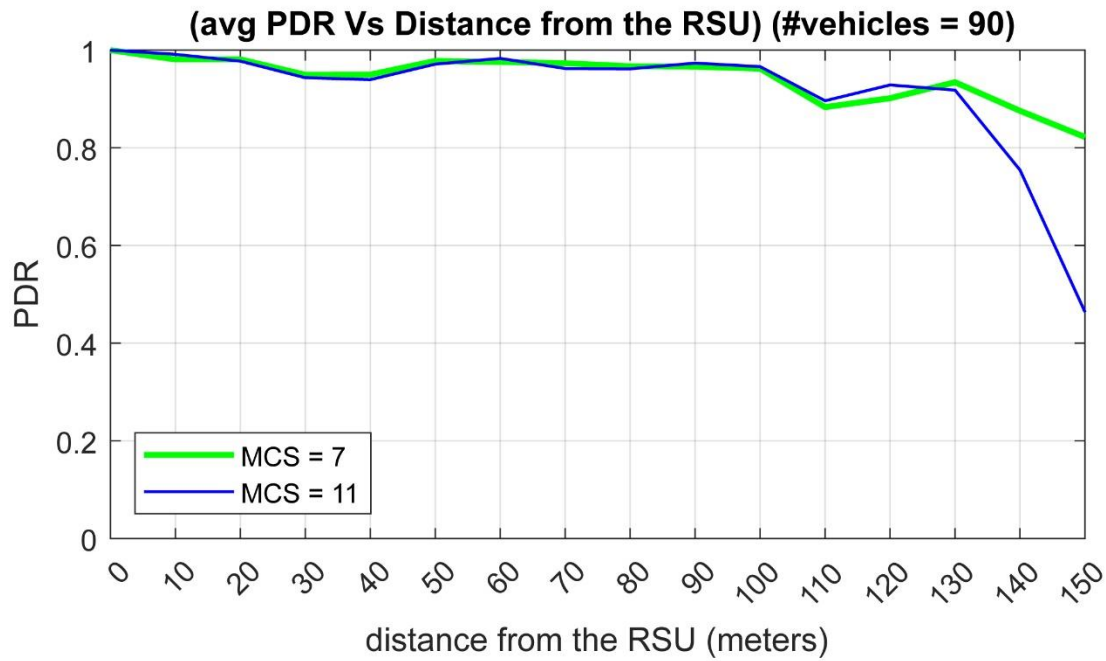
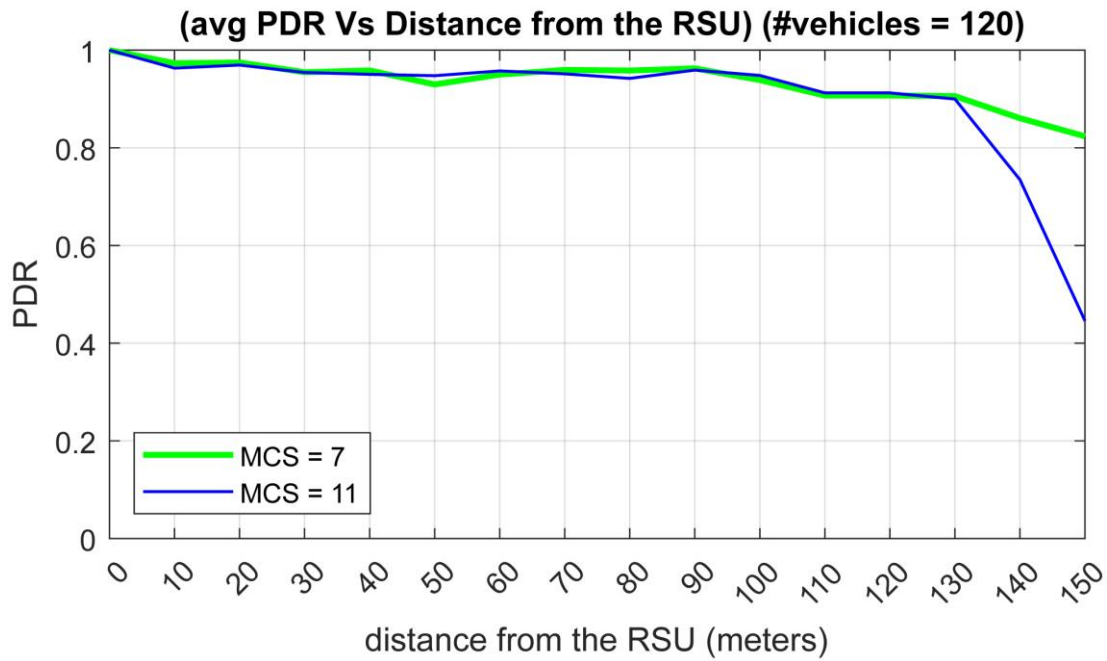
(a) for $\lambda = 15$ (b) for $\lambda = 20$

Figure 26. PDR Variation for $\lambda = \{15, 20\}$ with Respect to Distance from the RSU where Green Plots Indicate MCS 7 and Blue Plots Indicate MCS 11

CHAPTER 5

CONCLUSION AND FUTURE WORK

This research introduces a comprehensive computer simulation framework that integrates geographical and traffic configurations with the physical (PHY) and radio resource control (RRC) layers of the C-V2X system. The primary motivation for this study sprung from the recent decision by the U.S. federal government to allocate only 30 MHz of spectrum for V2X communication and the need to assess the impact of prevalent obstacles like building blocks and trailer trucks in a city road environment. Consequently, this investigation identified critical V2X safety messages and their corresponding applications, assessing whether they remain supported within the reduced bandwidth constraints and the presence of the obstacles. In an urban Mode 4 environment with Congestion Control Mechanism (CCM) enabled, the majority of safety-critical applications appeared to meet their latency requirements satisfactorily. Moreover, our C-V2X simulation successfully captured subtle performance distinctions influenced by key factors such as modulation and coding schemes (MCS). With the results and findings, it can be asserted with confidence that the fundamental PDR requirements are also maintained, even in situations of heightened traffic density.

In our future endeavors, we aim to enhance this simulator suite to encompass an expanded array of C-V2X capabilities, road conditions, and traffic scenarios. This includes but is not limited to accommodating functionalities such as NR-V2X, exploring mode 3 settings, and simulating scenarios like suburban highways. By broadening the scope of our simulator, we seek to provide a more comprehensive platform for evaluating C-V2X performance across diverse environments and operational conditions. This expansion will

enable researchers and practitioners to gain deeper insights into the behavior and efficacy of C-V2X systems in a wider range of real-world scenarios, ultimately contributing to the advancement and optimization of connected vehicle technologies.

REFERENCES

- © [2023] IEEE. Reprinted, with permission, from D. Sunuwar, S. Kim and Z. Reyes. Is 30 MHz Enough for C-V2X?. 2023 IEEE 98th Vehicular Technology Conference (VTC2023-Fall), Dec 2023.
- Hope Bovenzi. 2019. How Connected Vehicles Leverage Data: 3 Common Questions. Texas Instruments. <https://www.ti.com/document-viewer/lit/html/SSZT418>.
- U.S. Department of Transportation. 2017. Vehicle-to-vehicle communication technology. V2V Fact Sheet. Accessed 2024.
<https://www.nhtsa.gov/sites/nhtsa.dot.gov/files/documents/v2vfactsheet101414v2a.pdf>
- U.S. FCC. 2019. In the matter of use of the 5.850-5.925 GHz band. Notice of Proposed Rulemaking: ET Docket No. 19-138. FCC 19-129.
- T. ElBatt, S. Goel, G. Holland, H. Krishnan, and J. Parikh. 2006. Cooperative collision warning using dedicated short range wireless communications. ACM VANET.
- L. Cao, S. Roy, and H. Yin. 2022. Resource allocation in 5G platoon communication: Modeling, analysis and optimization. IEEE Trans. Veh. Technol.
- R. Wei. 2022. Performance analysis of semi-persistent scheduling throughput in 5G NR-V2X: A MAC perspective. arXiv:2208.10653v1.
- M. Akdeniz, Y. Liu, M. Samimi, S. Sun, S. Rangan, T. Rappaport, and E. Erkip. 2014. Millimeter wave channel modeling and cellular capacity evaluation. IEEE J. Sel. Areas Commun. 32(6).

- C. Zoghalmi, R. Kacimi, and R. Dhaou. 2022. 5G-enabled V2X communications for vulnerable road users safety applications: A review. Wireless Netw. 23.
- S. Sabeeh, K. Wesolowski, P. Sroka. 2022. C-V2X Centralized Resource Allocation with Spectrum Re-Partitioning in Highway Scenario. Electronics. 11(2):279. <https://doi.org/10.3390/electronics11020279>.
- S. K. Gupta, J. Y. Khan, and D. T. Ngo. 2019. An LTE-Direct-Based Communication System for Safety Services in Vehicular Networks. <https://www.intechopen.com/chapters/72121>.
- M. Gonzalez-Martín, M. Sepulcre, R. Molina-Masegosa, and J. Gozalvez. 2018. Analytical Models of The Performance of C-V2X Mode 4 Vehicular Communications. IEEE Transactions on Vehicular Technology: 1155–1166.
- R. Molina-Masegosa and J. Gozalvez. 2017. System Level Evaluation of LTE-V2V mode 4 Communications and its Distributed Scheduling. IEEE 85th Vehicular Technology Conference (VTC Spring): 1–5.
- C. Ghodhbane, M. Kassab, S. Maaloul, H. Aniss, M. Berbineau. 2022. A Study of LTE-V2X Mode 4 Performances in a Multiapplication Context. IEEE Access: 63579-63591.
- A. Mansouri, V. Martinez and J. Härrri. 2019. A First Investigation of Congestion Control for LTE-V2X Mode 4. 2019 15th Annual Conference on Wireless On-demand Network Systems and Services (WONS): 56-63. <https://ieeexplore.ieee.org/document/8795500>.
- ETSI TR 1389010 V17.0.0. 2022. 5G; Study on channel model for frequencies from 0.5 to 100 GHz. 3GPP.

- A. Bazzi, G. Cecchini, M. Menarini, B. Masini, A. Zanella. 2019. Survey and Perspectives of Vehicular Wi-Fi versus Sidelink Cellular-V2X in the 5G Era. Future Internet 11: 122.
- J3161/1A. 2022. Vehicle level validation test procedures for V2V safety communications. SAE.
- ETSI TS 123303 V17.0.0. 2022. Universal Mobile Telecommunications System (UMTS); LTE; Proximity-based services (ProSe); Stage 2. 3GPP.
- J2735. 2020. V2X communications message set dictionary. SAE.
- U.S. DOT. CV273: Introduction to SPaT / MAP messages. Module 62 - CV273. Accessed 2024. <https://www.pcb.its.dot.gov/standardstraining/mod62/ppt/m62ppt.htm>
- M. Garcia, A. Molina-Galan, M. Boban, J. Gozalvez, B. Coll-Perales, T. Sahin, and A. Kousaridas. 2021. A tutorial on 5G NR V2X communication. IEEE Commun. Surveys Tutorials.
- ETSI TS 122186, V17.0.0. 2022. 5G; Service requirements for enhanced V2X scenarios. 3GPP.
- A. Nabil, K. Kaur, C. Dietrich and V. Marojevic. 2018. Performance Analysis of Sensing-Based Semi-Persistent Scheduling in C-V2X Networks. IEEE 88th Vehicular Technology Conference (VTC-Fall):1- 5.
- T. Karunathilake and A. Forster. 2022. A survey on mobile road side units in VANETs. MDPI Veh. 4(2).

ETSI TS 136101, V15.20.0. 2023. LTE; Evolved Universal Terrestrial Radio Access (E-UTRA); User equipment (UE) radio transmission and reception. 3GPP.

ETSI TR 137985, V16.0.0. 2022. LTE; 5G Overall description of Radio Access Network (RAN) aspects for Vehicle-to-everything (V2X) based on LTE and NR. 3GPP.

ETSI TS 136213, V15.16.0. 2022. LTE; Evolved Universal Terrestrial Radio Access (E-UTRA); Physical layer procedures. 3GPP.

ETSI TS 103574, V1.1.1. 2018. Intelligent Transport Systems (ITS); Congestion Control Mechanisms for the C-V2X PC5 interface; Access layer part. 3GPP.

C. Ghodhbane, M. Kassab, S. Maaloul, H. Aniss and M. Berbineau. 2022. A Study of LTE-V2X Mode 4 Performances in a Multiapplication Context," in IEEE Access: 10(63579-63591). <https://ieeexplore.ieee.org/document/9794751>